

# Water Resources Research

## RESEARCH ARTICLE

10.1029/2022WR032522

### Key Points:

- Shallow lakes and ponds are assumed to be well mixed, yet we identified three mixing regimes: rarely, intermittently, or often mixed
- Across 34 temperate shallow lakes and ponds, mixing regimes were primarily regulated by surface area and depth
- Small, shallow waters mix due to shortwave radiation and convection; large, shallow waters mix due to wind

### Supporting Information:

Supporting Information may be found in the online version of this article.

### Correspondence to:

M. A. Holgerson,  
meredith.holgerson@cornell.edu

### Citation:

Holgerson, M. A., Richardson, D. C., Roith, J., Bortolotti, L. E., Finlay, K., Hornbach, D. J., et al. (2022). Classifying mixing regimes in ponds and shallow lakes. *Water Resources Research*, 58, e2022WR032522. <https://doi.org/10.1029/2022WR032522>

Received 5 APR 2022

Accepted 1 JUL 2022

### Author Contributions:

**Conceptualization:** Meredith A. Holgerson, David C. Richardson  
**Data curation:** Meredith A. Holgerson, David C. Richardson, Joseph Roith, Kshitij Gurung, Andrew Ness  
**Formal analysis:** Meredith A. Holgerson, David C. Richardson, Joseph Roith  
**Investigation:** Meredith A. Holgerson, David C. Richardson, Joseph Roith, Lauren E. Bortolotti, Kerri Finlay, Daniel J. Hornbach, Kshitij Gurung, Andrew Ness, Mikkel R. Andersen, Sheel Bansal, Jacques C. Finlay, Jacob A. Cianci-Gaskill, Shannon Hahn, Benjamin D. Janke, Cory McDonald, Jorrit P. Mesman

© 2022 The Authors.

This is an open access article under the terms of the Creative Commons Attribution-NonCommercial License, which permits use, distribution and reproduction in any medium, provided the original work is properly cited and is not used for commercial purposes.

## Classifying Mixing Regimes in Ponds and Shallow Lakes

Meredith A. Holgerson<sup>1</sup> , David C. Richardson<sup>2</sup> , Joseph Roith<sup>3</sup>, Lauren E. Bortolotti<sup>4</sup> , Kerri Finlay<sup>5</sup> , Daniel J. Hornbach<sup>6</sup> , Kshitij Gurung<sup>3</sup>, Andrew Ness<sup>3</sup>, Mikkel R. Andersen<sup>7</sup> , Sheel Bansal<sup>8</sup> , Jacques C. Finlay<sup>9</sup> , Jacob A. Cianci-Gaskill<sup>10</sup> , Shannon Hahn<sup>6</sup>, Benjamin D. Janke<sup>9</sup> , Cory McDonald<sup>11</sup>, Jorrit P. Mesman<sup>12,13</sup> , Rebecca L. North<sup>10</sup> , Cassandra O. Roberts<sup>14</sup> , Jon N. Sweetman<sup>15</sup> , and Jackie R. Webb<sup>16</sup> 

<sup>1</sup>Department of Ecology and Evolutionary Biology, Cornell University, Ithaca, NY, USA, <sup>2</sup>Biology Department, SUNY New Paltz, New Paltz, NY, USA, <sup>3</sup>Department of Mathematics, Statistics, and Computer Science, St. Olaf College, Northfield, MN, USA, <sup>4</sup>Institute for Wetland and Waterfowl Research, Ducks Unlimited Canada, Stonewall, MB, Canada, <sup>5</sup>Department of Biology, University of Regina, Regina, SK, Canada, <sup>6</sup>Department of Environmental Studies, Macalester College, St. Paul, MN, USA, <sup>7</sup>Centre for Freshwater and Environmental Studies, Dundalk Institute of Technology, Dundalk, Ireland, <sup>8</sup>U.S. Geological Survey, Northern Prairie Wildlife Research Station, Jamestown, ND, USA, <sup>9</sup>Department of Ecology, Evolution and Behavior, University of Minnesota, Saint Paul, MN, USA, <sup>10</sup>School of Natural Resources, University of Missouri-Columbia, Columbia, MO, USA, <sup>11</sup>Department of Civil, Environmental, and Geospatial Engineering, Michigan Technological University, Houghton, MI, USA, <sup>12</sup>Department F.A. Forel for Environmental and Aquatic Sciences, University of Geneva, Geneva, Switzerland, <sup>13</sup>Department of Ecology and Genetics, Uppsala University, Uppsala, Sweden, <sup>14</sup>School of Sciences, Elizabethtown College, Elizabethtown, PA, USA, <sup>15</sup>Department of Ecosystem Science and Management, Penn State University, State College, PA, USA, <sup>16</sup>Centre for Regional and Rural Futures (CeRRF), Faculty of Science, Engineering and Built Environment, Deakin University, Burwood, NSW, Australia

**Abstract** Lakes are classified by thermal mixing regimes, with shallow waterbodies historically categorized as continuously mixing systems. Yet, recent studies demonstrate extended summertime stratification in ponds, underscoring the need to reassess thermal classifications for shallow waterbodies. In this study, we examined the summertime thermal dynamics of 34 ponds and shallow lakes across temperate North America and Europe to categorize and identify the drivers of different mixing regimes. We identified three mixing regimes: rarely ( $n = 18$ ), intermittently ( $n = 10$ ), and often ( $n = 6$ ) mixed, where waterbodies mixed an average of 2%, 26%, and 75% of the study period, respectively. Waterbodies in the often mixed category were larger ( $\geq 4.17$  ha) and stratification weakened with increased wind shear stress, characteristic of “shallow lakes.” In contrast, smaller waterbodies, or “ponds,” mixed less frequently, and stratification strengthened with increased shortwave radiation. Shallow ponds ( $<0.74$  m) mixed intermittently, with daytime stratification often breaking down overnight due to convective cooling. Ponds  $\geq 0.74$  m deep were rarely or never mixed, likely due to limited wind energy relative to the larger density gradients associated with slightly deeper water columns. Precipitation events weakened stratification, even causing short-term mixing (hours to days) in some sites. By examining a broad set of shallow waterbodies, we show that mixing regimes are highly sensitive to very small differences in size and depth, with potential implications for ecological and biogeochemical processes. Ultimately, we propose a new framework to characterize the variable mixing regimes of ponds and shallow lakes.

## 1. Introduction

Lakes have historically been classified based on mixing regimes (Hutchinson & Loeffler, 1956; Lewis Jr., 1983) as mixing frequency drives key ecosystem processes, including benthic oxygen availability, sediment resuspension, nutrient and carbon recycling, and greenhouse gas production and emissions (Andersen et al., 2019; Mesman et al., 2021; Vachon et al., 2019; Wilhelm & Adrian, 2007). While mixing patterns in deepwater lakes are well established (Hutchinson & Loeffler, 1956), shallow waterbodies have more complex mixing regimes that still need resolution. Lewis Jr. (1983) first incorporated shallow waterbodies into thermal mixing regimes, proposing four polymictic (i.e., mixing several times per year) categories based on whether systems were cold (ice covered at any time of year) or warm (no ice cover) and if mixing was continuous (daily) or discontinuous (not occurring every day). Lewis Jr. (1983) suggested that the boundary between continuous and discontinuous mixing was  $\sim 20$  m deep at a 25 km fetch, with a shallower boundary as fetch decreased. This work prompted the assumption that all shallow lentic waterbodies are well mixed (Branco & Torgersen, 2009; Choffel et al., 2017; Scheffer, 2004), which may be incorrect. While some shallow waterbodies do mix continuously for much of the summer (Torremorell



Rebecca L. North, Cassandra O. Roberts, Jon N. Sweetman, Jackie R. Webb

**Methodology:** Meredith A. Holgerson, David C. Richardson, Joseph Roith

**Project Administration:** Meredith A. Holgerson

**Resources:** Meredith A. Holgerson, David C. Richardson, Lauren E. Bortolotti, Kerri Finlay, Daniel J.

Hornbach, Mikkel R. Andersen, Sheel Bansal, Jacques C. Finlay, Jacob A. Cianci-Gaskill, Cory McDonald, Jorrit P. Mesman, Rebecca L. North, Jon N. Sweetman

**Supervision:** Meredith A. Holgerson, Joseph Roith

**Validation:** Meredith A. Holgerson, David C. Richardson, Joseph Roith

**Visualization:** Meredith A. Holgerson, David C. Richardson, Joseph Roith

**Writing – original draft:** Meredith A. Holgerson, David C. Richardson, Joseph Roith

**Writing – review & editing:** Meredith A. Holgerson, David C. Richardson, Joseph Roith, Lauren E. Bortolotti, Kerri Finlay, Daniel J. Hornbach, Kshitij Gurung, Andrew Ness, Mikkel R. Andersen, Sheel Bansal, Jacques C. Finlay, Jacob A. Cianci-Gaskill, Shannon Hahn, Benjamin D. Janke, Cory McDonald, Jorrit P. Mesman, Rebecca L. North, Cassandra O. Roberts, Jon N. Sweetman, Jackie R. Webb

et al., 2007), others stratify for days to weeks at a time (Andersen et al., 2019; Holgerson et al., 2016; Martinsen et al., 2019) indicating a much shallower threshold for discontinuous mixing than proposed by Lewis Jr. (1983). Assuming shallow waterbodies to be well mixed when they actually spend much of the time stratified obscures important ecosystem processes. As shallow waterbodies are globally abundant and increasingly recognized for their active role in global biogeochemical cycling (Downing, 2010; Holgerson & Raymond, 2016; Schmadel et al., 2019), it is critical to understand their mixing and stratification patterns.

The stratification and mixing regimes of a waterbody reflect its heat budget, which differs in smaller, shallower waterbodies compared to larger, deeper lakes. Stratification occurs when insolation exceeds heat loss; conversely, turbulence generated from heat loss and wind shear deepens the mixed layer and destabilizes the water column (MacIntyre & Melack, 2010). Deeper waters have a higher heat capacity and can stratify more strongly than shallow waters (Magee & Wu, 2017), and larger waters have more turbulence due to wind shear compared to smaller, sheltered systems where turbulence is driven by convection (Read et al., 2012). As a result, the boundary between whether a waterbody is mixed or stratified increases as a function of increasing area and depth (Gorham & Boyce, 1989; Kirillin & Shatwell, 2016; Lathrop & Lillie, 1980). While smaller waterbodies on the scale of a few hectares or less (commonly referred to as “ponds”; Richardson et al., 2022) have been excluded from these predictive frameworks, surface area and depth may similarly regulate mixing. For instance, large and shallow lakes may mix frequently, whereas ponds may often stratify due to sheltering from the surrounding topography and vegetation (Andersen et al., 2017; Chimney et al., 2006; Markfort et al., 2010). Yet, the interaction between surface area, depth, and mixing frequency remains unresolved in shallow waterbodies.

While surface area and depth are the primary factors driving mixing regimes, greater light attenuation (i.e., decreased water transparency) can also influence mixing by decreasing mixing depth and strengthening stratification (Bukaveckas & Driscoll, 1991; Hocking & Straskraba, 1999; Mazumder & Taylor, 1994). In shallow systems, where light has the potential to reach a greater proportion of the water column, changes in light attenuation can have particularly strong effects on mixing (Fee et al., 1996; Mesman et al., 2021). For example, increases in dissolved organic carbon (DOC) concentration (Brothers et al., 2014) and phytoplankton biomass (Shatwell et al., 2016) each reduce transparency and can cause well-mixed lakes to stratify for large periods of the summer. Aquatic macrophytes can also strengthen stratification by increasing light attenuation and reducing wind speed and underwater turbulence, playing a larger role in shallower waterbodies where macrophytes can colonize much of the surface area (Andersen et al., 2017; Herb & Stefan, 2004; Sand-Jensen et al., 2019).

Climate and weather also influence mixing patterns. Latitude and elevation were central to the first lake mixing classifications (Hutchinson & Loeffler, 1956; Lewis Jr., 1983). At finer scales, local weather affects solar radiation reaching a waterbody and internal turbulence generated from heat loss, wind, and precipitation. Episodic meteorological events (i.e., storms) can impact lake stability due to increased wind and precipitation, which can induce partial or complete mixing in stratified lakes (Jennings et al., 2012; Kasprzak et al., 2017; Klug et al., 2012). We expect different effects in smaller and shallower waterbodies where weak stratification can persist (Doubek et al., 2021) and a deepening of the thermocline can result in complete mixing to the sediment. We also expect that precipitation can have more pronounced effects on ponds where the precipitation volume relative to the water volume is much higher than in deeper, larger lakes. For instance, small and shallow ponds can double in water depth following heavy rainfall (Holgerson, 2015), which may initially increase mixing but could result in more stable stratification over time due to deeper waters. Identifying how precipitation events affect mixing in shallow waters is particularly important as we expect mixing dynamics to shift in response to climatic and environmental change (Bartosiewicz et al., 2019; Mesman et al., 2021; Woolway & Merchant, 2019).

We currently lack a framework to describe mixing patterns in globally abundant shallow waterbodies, thus limiting our understanding of ecosystem structure and function (Andersen et al., 2017; Mesman et al., 2021; Sand-Jensen et al., 2019). This study provides the first examination of mixing regimes across a broad range of 34 shallow lakes and ponds in North America and Europe in order to (a) quantitatively categorize mixing regimes and (b) identify the drivers of different mixing regimes. We predicted that mixing regimes would vary from mostly mixed to mostly stratified, and would relate primarily to surface area and depth, with secondary importance from light attenuation, vegetation, water chemistry, and weather events.

**Table 1**  
*Physical, Chemical, and Biological Parameters of the 34 Waterbodies Throughout North America and Europe*

Variable	n	Range	Mean	Median
Latitude (°)	34	38.9 – 54.0	46.1	45.0
Surface area (ha)	34	0.02 – 823.00	26.86	0.32
Perimeter (m)	29	77 – 11,070	816	250
Fetch (m)	34	22 – 3,190	261	89
Maximum depth (m)	34	0.47 – 4.20	1.58	1.33
Mean depth (m)	16	0.30 – 1.87	0.97	0.86
DOC (mg L <sup>-1</sup> )	25	5.0 – 32.5	14.9	14.0
TP (µg L <sup>-1</sup> )	17	18.6 – 1,871.0	312.2	188.8
TDP (µg L <sup>-1</sup> )	11	25.9 – 684.4	200.6	131.6
Chlorophyll <i>a</i> (µg L <sup>-1</sup> )	21	2.7 – 147.8	38.1	28.1
Conductivity (µS cm <sup>-1</sup> )	30	8.0 – 5,282.0	614.5	243.9
pH	29	4.5 – 9.2	7.3	7.4
$K_D$ (m <sup>-1</sup> )	19	2.1 – 14.9	5.1	4.1
Emergent vegetation cover (%)	31	0 – 93	16	10
Submerged vegetation cover (%)	32	0 – 95	29	9
Floating vegetation cover (%)	33	0 – 100	31	10

*Note.* Sample sizes (n) represent the number of ponds sampled for each variable. DOC = dissolved organic carbon, TP = total phosphorus, TDP = total dissolved phosphorus, and  $K_D$  = light attenuation.

## 2. Methods

### 2.1. Study Sites

We studied 34 waterbodies throughout North America and Europe (Figure S1 in Supporting Information S1), with all sites located in temperate ecoregions (Olson & Dinerstein, 2002). All waterbodies were shallow (range: 0.47 – 4.2 m; Table 1), and most were small (median: 0.32 ha; range: 0.02–823 ha; Table 1). Most waterbodies were small and shallow enough to be considered “ponds,” which tend to be <5 ha in size (Biggs et al., 2005; Oertli et al., 2005, 2009; Richardson et al., 2022), and we also included several larger and shallow waterbodies, representative of “shallow lakes” (Scheffer, 2004). We included a size gradient in order to capture potential shifts in mixing patterns that could help to functionally differentiate ponds and shallow lakes (Fairchild et al., 2005).

### 2.2. Field Sampling

Waterbodies were sampled during the open-water period between 2013 and 2020; only one season of data was used per waterbody. We recorded water temperatures using multiple thermistors that spanned the water column near the waterbody’s maximum depth. While the exact deployment setup differed among sites (Table S1 in Supporting Information S1), each waterbody had a minimum of three thermistors to record benthic and surface temperature along with at least one mid-water column temperature, and most waterbodies had additional sensors (mean: 5, max: 8). Thermistors recorded water temperature every 10 – 30 min (Table S1 in Supporting Information S1). For sites where depth fluctuated, we monitored changes over time manually or using pressure transducers.

We measured the physical, chemical, and biological characteristics of each study site at least once during the study period (Table 1). Measurements included maximum depth, surface area, perimeter, fetch (longest axis), pH, conductivity, DOC, total phosphorus (TP) and/or total dissolved phosphorus (TDP), chlorophyll *a*, light attenuation ( $K_D$ ), and the percent cover of emergent, submerged, and floating macrophytes. We estimated  $K_D$  from either water column profiles of photosynthetically active radiation (PAR) or using recently deployed light sensors (prior to any biofouling) measuring illuminance in lux. We converted lux to PAR based on Long et al. (2012), and calculated  $K_D$  as the slope of a linear regression model of PAR (natural log) versus depth. We measured on-site

meteorological data at a subset of waterbodies, including wind speed, precipitation, and air temperature; the data for remaining sites were compiled from local meteorological stations (Table S1 in Supporting Information S1).

### 2.3. Quality Assurance

We conducted quality assurance checks for each waterbody by (a) plotting water temperatures for all sensors through time, and (b) creating heatmaps interpolating water column temperatures through time using the *R* rLakeAnalyzer package (Winslow et al., 2019), which we modified to allow depth to fluctuate. All quality assurance checks and statistical analyses hereafter were performed in *R* (R Core Team, 2020). We identified and removed any irregular data, such as periods where the sensors were out of the water (large temperature swings) or submerged in sediments (limited temperature change). Density plots and heat maps can be interactively explored online ([https://jroith.shinyapps.io/Ponds\\_Plot\\_Dashboard/](https://jroith.shinyapps.io/Ponds_Plot_Dashboard/)) using the shiny dashboard (Chang et al., 2021) and static plots are provided in the supplement (Figure S8 in Supporting Information S1).

### 2.4. Classifying Mixing Versus Stratification

To determine mixing and stratification dynamics, we examined differences in water density gradients between the top and bottom of the water column. We calculated water density from water temperature using the rLakeAnalyzer package (Winslow et al., 2019). Density calculations assumed freshwater (salinity = 0) as we lacked conductivity or salinity water column profiles for most sites. While this assumption likely holds for most of our study sites, waterbodies near roads, within agricultural, or within urban landscapes could develop salinity gradients which might facilitate stratification (Ladwig et al., 2021). We compared the water density from the deepest and shallowest sensors and divided by the distance separating the two sensors to create a density gradient in units of  $\text{kg m}^{-3} \text{ m}^{-1}$ . Density gradients are commonly used to examine mixed layer depth (Gray et al., 2020); however, other parameters can also be used to examine stratification and mixing (e.g., buoyancy frequency, Schmidt stability; Read et al., 2011). As density gradient, buoyancy frequency, and Schmidt stability performed similarly in three ponds with different mixing regimes (Figures S2 – S4 in Supporting Information S1), we used density gradients to maximize the number of study sites since we did not have bathymetry data for all waterbodies.

To exclude seasonal impacts on mixing, we focused our data analysis on a summer period when thermal stratification was potentially at its maximum. For each waterbody, we determined the day of year when the density gradient was the highest and took the median value across all sites (10 July). We established a date range of 30 days before and after 10 July to include in our analysis to exclude sampling that may incorporate transitional season mixing at higher latitudes. This range (10 June – 9 August) included the maximum density gradient for 28/34 waterbodies (82%), with 33/34 waterbodies (97%) reaching over 85% of their recorded maximum density gradient value during this period. The one remaining site (Pond E1) had the maximum density gradient on 8 June (2 days before our cutoff). Our analysis only included sites with a minimum of 21 unique, but not necessarily sequential, days within this time window.

To classify ponds as mixed or stratified at a given time point, we examined different possible density gradient thresholds, which vary in the literature from 0.03 to 0.50  $\text{kg m}^{-3} \text{ m}^{-1}$  (see Gray et al., 2020). We calculated the proportion of time each waterbody mixed during the day, night, and combined for thresholds ranging from 0.000 to 0.400  $\text{kg m}^{-3} \text{ m}^{-1}$  by increments of 0.001  $\text{kg m}^{-3} \text{ m}^{-1}$ . We conducted a *k*-means clustering analysis to evaluate whether waterbodies grouped together based on the proportion of time mixed during the day and night. Across thresholds, we identified the mixing regime clusters that performed the best (lowest within sum of squares), with all clusters having  $n > 1$  waterbodies. To select a density gradient threshold for further analyses, we ran a sensitivity analysis to examine all possible mixing thresholds and selected the threshold that explained the greatest proportion of variance for the clusters.

### 2.5. Analyzing Drivers of Mixing Regimes

We examined the time of day when mixing occurred in each cluster using a subset of sites that mixed at least once during the entire study period ( $n = 26$  waterbodies). To establish the time when the mixing event began, we identified any time of day that the density gradient crossed from above the threshold to below. These times were converted to seconds past midnight (considering the local time zone) using the lubridate package in *R* (Spinu

et al., 2021) and analyzed using a Kruskal-Wallis test to compare the time of day mixing occurred among the three clusters. Results were transformed back to time of day on a 24 hr scale to interpret when mixing began among the clusters.

We examined the relationship between environmental variables (Table 1) and the mixing regime clusters using analysis of variance (ANOVA) and examined pairwise differences with Tukey's honestly significant difference (HSD) tests. To examine which environmental variables predicted the mixing regime clusters, we used classification and regression tree (CART) analysis using the rpart package in *R* (Therneau et al., 2019). Prior to the CART analysis, we examined correlations among possible predictor variables after transforming any variables with strongly non-normal distributions (Table S3 in Supporting Information S1). Due to both collinear variables with similar predicted effects on mixing (e.g., surface area, perimeter, and fetch) and a limited sample size relative to the possible number of predictor variables, we built our classification tree with a subset of environmental variables: surface area, maximum depth, DOC, chlorophyll *a*, percent submerged vegetative cover, percent floating vegetative cover, and percent emergent vegetative cover. When we substituted out collinear variables in the CART model, the pruned tree remained the same. Trees were fit using a complexity parameter of 0.01, minimum bucket size of three, and minimum split of two. We pruned the tree based on the minimum classification error.

We evaluated the relationship between three daily meteorological-related variables that drive surface water energetic exchange (sum of shortwave radiation, maximum wind shear stress, and mean convective heat transfer) and the mean daily density gradient for each waterbody. Hourly weather data were downloaded from two different reanalysis data sources: the North American Land Data Assimilation System (NLDAS-2, Xia et al., 2012) and the European Center for Medium-Range Weather Forecast European ReAnalysis (ECMWF ERA5, Muñoz-Sabater et al., 2021). Shortwave radiation (SW radiation) is the daily sum of shortwave radiation ( $\text{W m}^{-2}$ ). Wind shear stress was calculated from Read et al. (2011):

$$\tau = C_d \rho_A U^2 \quad (1)$$

where  $\tau$  is the wind shear stress ( $\text{N m}^{-2}$ ),  $C_d$  is the dimensionless drag coefficient (0.001 if wind speed  $< 5 \text{ m s}^{-1}$ , 0.0015 otherwise),  $\rho_A$  is the air density ( $\text{kg m}^{-3}$ ), and  $U$  is the wind speed at 10 m ( $\text{m s}^{-1}$ ). Convective heat transfer was calculated using Newton's Law of Cooling:

$$Q_{\text{conv}} = h (T_{\text{air}} - T_{\text{water}}) \quad (2)$$

where  $Q_{\text{conv}}$  is the heat transferred by convection ( $\text{W m}^{-2}$ ),  $h$  is the heat transfer coefficient ( $\text{W m}^{-2} \text{°C}^{-1}$ ),  $T_{\text{air}}$  is the air temperature at 10 m ( $^{\circ}\text{C}$ ), and  $T_{\text{water}}$  is the surface water temperature ( $^{\circ}\text{C}$ ). The heat transfer coefficient,  $h$ , was calculated as a constant ( $17.5 \text{ W m}^{-2} \text{ °C}^{-1}$ , Singh et al., 1994) or as a function of wind speed ( $2.8 + 3.0U$ , Watmuff et al., 1977). Because of a high degree of correlation between the two convective heat transfers ( $r = 0.97$ ,  $p < 0.001$ ), we used the constant calculation to isolate heat transfer from wind shear stress. We acknowledge that our  $Q_{\text{conv}}$  and  $h$  terms are simplistic and they would be more accurately characterized by calculating heat budgets (MacIntyre et al., 2010; Read et al., 2012; Woolway et al., 2015) with required data that were not available for most of our waterbodies.

For each waterbody, we calculated z-scores for all three meteorological-related energy transfer variables to standardize comparisons. We calculated the relationship between the density gradient and each energy transfer variables simultaneously by fitting regression coefficients ( $\beta$ ) and modeled the residuals using the auto.arima function in the *R* forecast package which fits the best AutoRegressive Integrated Moving Average (ARIMA) model based on minimizing AICc values (Hyndman et al., 2021). We calculated whether each  $\beta$  was significantly different from 0 using a one-sample *t*-test and Holm-corrected *p*-values for the multiple comparisons across all sites with family  $\alpha = 0.05$ . Based on the results from the ARIMA time series analysis, we investigated whether geomorphological characteristics (maximum depth and surface area) could predict which waterbodies were most responsive to solar radiation, wind shear stress, and heat transfer for mixing regime clusters using linear regression models. We examined the relationship between both morphological variables with each  $\beta$  using either simple linear regression or exponential model fit, selecting the model with the lowest AICc.

We identified large precipitation events as those that had more than 25.4 mm (1 inch) of precipitation on any single day; this daily total precipitation generally exceeds the 90th percentile for temperate regions (Palecki et al., 2005). To isolate the effect of single precipitation events, we selected days with large precipitation events

( $>25.4$  mm) that had only minimal precipitation ( $<25.4$ ) on the preceding or following day, resulting in 30 large precipitation events across all sites. We examined the daily averages of the density gradient from the day before the event (day = -1), the day of the event (day = 0), to the day after the event (day = 1) using the mean daily density gradient. To standardize across events, we used the percent change in density gradient from the day preceding the precipitation event to each of the next 2 days. For the day of the precipitation event and the day after the precipitation event, we compared the percent change in density gradient between clusters using a non-parametric Kruskal-Wallis test.

To determine if waterbodies across the landscape responded synchronously to precipitation, we identified a 2 day precipitation event (30 June–01 July 2019) impacting 12 study sites in southeastern Minnesota, USA. This precipitation event was not included in the prior analysis because of the two consecutive days of precipitation. We used precipitation data collected at the Katharine Ordway Natural History Study Site, which is centrally located and  $<50$  km from the 12 waterbodies. We examined density gradient patterns over 6 days (28 June–03 July 2019) with 2 days preceding, 2 days during, and 2 days following the precipitation event. We analyzed the change in daytime maximum density gradients during the 2 days of precipitation events and the 2 days after, relative to the maximums during the 2 days preceding the precipitation events.

### 3. Results

#### 3.1. Mixing Regimes

The 34 waterbodies exhibited a wide range of mixing conditions, from sites that never mixed to sites that mixed for most of the summer. Our clustering analysis identified three distinct mixing regimes, which were robust across a wide range of density thresholds (Figure 1, Figure S5 in Supporting Information S1). We found that the density thresholds of  $0.032$  and  $0.287$   $\text{kg m}^{-3} \text{ m}^{-1}$  each explained 92.1% of the variance in clusters. However,  $0.287$   $\text{kg m}^{-3} \text{ m}^{-1}$  appeared more stable, whereas  $0.032$   $\text{kg m}^{-3} \text{ m}^{-1}$  was immediately followed by a reduction in the proportion of deviance explained where multiple waterbodies switched clusters (Figure S5, Table S2 in Supporting Information S1). Across the entire threshold gradient from  $0.032$  to  $0.400$   $\text{kg m}^{-3} \text{ m}^{-1}$ , 74% of waterbodies did not change clusters (Table S2 in Supporting Information S1). Of the remaining nine waterbodies, only four switched clusters when the mixing threshold was  $\geq 0.100$   $\text{kg m}^{-3} \text{ m}^{-1}$  (Figure 1; Table S2 in Supporting Information S1). We therefore selected  $0.287$   $\text{kg m}^{-3} \text{ m}^{-1}$  as our mixing threshold (Figure 1c), and identified that 18 waterbodies mixed rarely or never, 10 mixed intermittently, and six mixed often.

Across clusters, we observed clear differences in mixing conditions via density gradients and water temperature patterns (Figure 2; Figures S5 and S6 in Supporting Information S1). Rarely mixed waterbodies were mixed for 2% of the study period on average (range: 0% – 13%) and were similarly stratified during day and night (Figure 1c). The rarely mixed category included eight waterbodies that never crossed the density threshold (Figures 2a and 2b) and ones with relatively few time points that crossed that threshold (Figures 2c and 2d). Intermittently mixed waterbodies were mixed 26% of the time on average (range: 17%–41%; Figure 1c), and daily stratification often weakened or broke down overnight (Figures 2e and 2f). Consequently, waterbodies were mixed 31% of the time at night, on average, compared to 24% of the daytime. Lastly, often-mixed systems were isothermal 75% of the time on average (range: 58% – 88%), with rare instances of stratification (Figures 2g and 2h). Mixing was the norm at night, occurring 86% of the time on average, compared to 69% of the time during the day (Figure 1c).

Clusters differed in the time of day when mixing occurred (Figure 3). The time at which mixing occurred was mid-afternoon (mean:  $14:20 \pm 06:12$  SD; mode: 16:30) in often mixed waterbodies, whereas it was morning in rarely mixed (mean:  $07:15 \pm 05:39$  SD; mode: 05:30) and intermittently mixed (mean:  $09:46 \pm 08:08$  SD; mode: 03:30) waterbodies. These times were all statistically significantly different (Kruskal-Wallis,  $\chi^2 = 96.32$ ,  $p < 0.01$ ,  $df = 2$ ).

#### 3.2. Environmental Predictors of Mixing Regimes

Mixing clusters were most strongly related to waterbody morphometry, as determined by both examining individual environmental predictor variables and using a predictive CART model. Often mixed waterbodies had greater surface area, perimeter, and fetch when compared to rarely or intermittently mixed sites (Tukey HSD,  $p < 0.01$ , Figure S7, Table S4 in Supporting Information S1). Rarely mixed waterbodies had a greater maximum depth (mean  $\pm$  SD:  $1.9 \pm 0.9$  m) than intermittently mixed sites ( $1.1 \pm 0.6$  m; Tukey HSD,  $p < 0.01$ ), with a similar

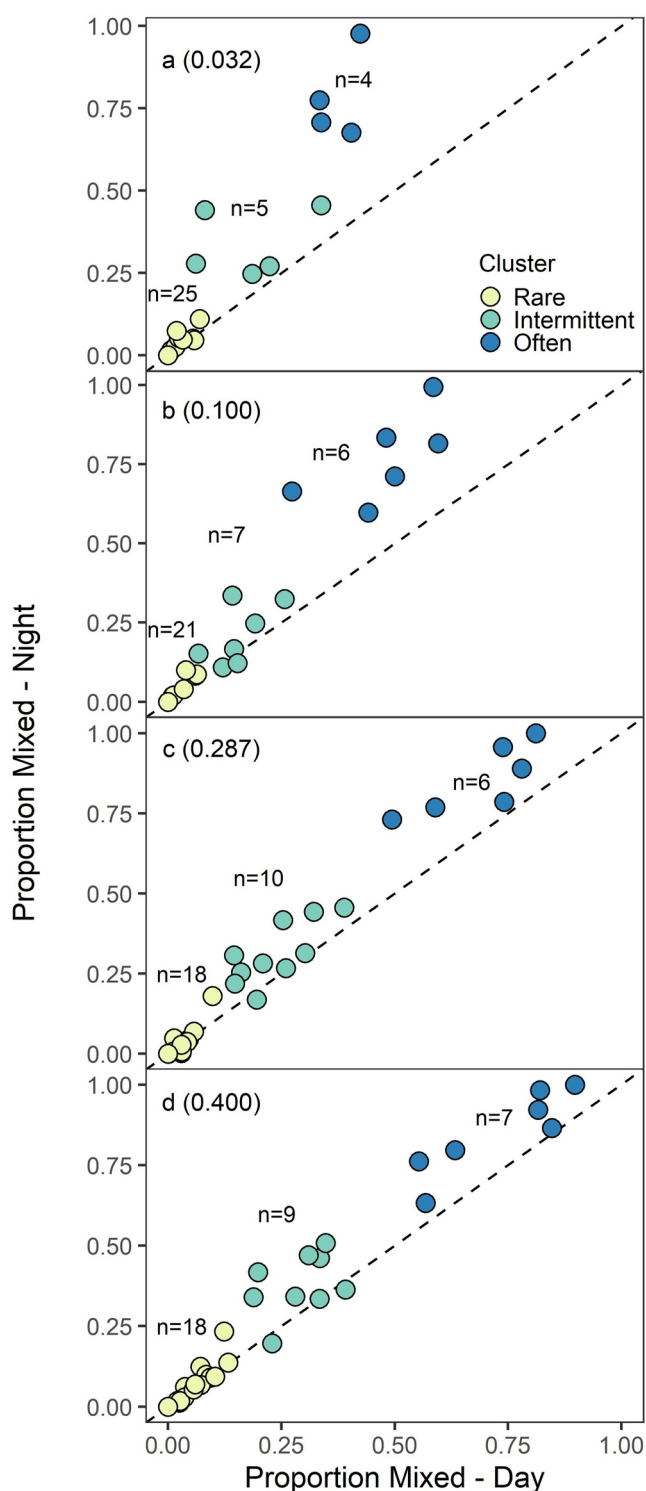


**Figure 1.** The proportion of time 34 waterbodies were mixed during the day and night were used to identify three mixing regimes (Rare = rarely mixed; Intermittent = intermittently mixed; Often = often mixed) using a cluster analysis across a range of density gradients from 0.000 to 0.400  $\text{kg m}^{-3} \text{m}^{-1}$ . Four examples are shown here: (a) 0.032, (b) 0.100, (c) 0.287, and (d) 0.400. Thresholds from (a and c) were identified from the sensitivity analysis, and (b and d) were selected to show the range of thresholds evaluated. The number of waterbodies in each cluster are identified on the figure. Dashed lines represent the 1:1 lines.

but non-statistically significant trend when compared to often mixed sites ( $1.1 \pm 0.4 \text{ m}$ ; Tukey HSD,  $p = 0.07$ ); mean depth was similar among the three clusters (ANOVA,  $F_{2,13} = 0.356$ ,  $p = 0.71$ ). For water chemistry, there were no significant differences in DOC, TP, or TDP among mixing clusters (ANOVA,  $p > 0.15$ ), although often mixed waterbodies had higher conductivity (Tukey HSD,  $p = 0.02$ ) and pH (Tukey HSD,  $p = 0.04$ ) than intermittently mixed sites, with a similar but weaker trend seen in comparison to rarely mixed sites (Tukey HSD,  $p < 0.10$ ). Chlorophyll *a* concentrations,  $K_D$ , and the percent coverage of submerged and emergent plants were all similar among the mixing clusters (ANOVA,  $p > 0.20$ ). However, often mixed waterbodies had less floating plant cover than rarely mixed sites (Tukey HSD,  $p = 0.05$ ), with a similar but weaker trend in comparison to intermittently mixed sites (Tukey HSD,  $p = 0.09$ ).

Surface area and maximum depth best predicted mixing cluster from the pruned regression tree (Figure 4a). The first split was based on surface area, where waterbodies  $\geq 4.17 \text{ ha}$  were often mixed. Mixing in waterbodies  $< 4.17 \text{ ha}$  was related to depth: sites  $< 0.74 - 2 \text{ m}$  mixed intermittently, sites between  $0.74 - 2 \text{ m}$  were hardest to classify but tended to mix rarely or intermittently, and sites  $> 2 \text{ m}$  rarely mixed (Figure 4b).

### 3.3. Daily Density Gradient and Meteorological Data

Of the three energy transfer variables we examined (shortwave radiation, wind shear stress, and convective heat transfer), shortwave radiation had the largest number of significant relationships (21/34) with daily density gradient and all were positive trends (Figure 5a). However, the significant relationships differed by cluster with 50% significant relationships in rarely mixed sites, 70% in intermittently mixed sites, and 83% in often mixed sites. Conversely, maximum daily wind shear stress had fewer significant relationships (11/34) and was negatively related to daily density gradients in most significant relationships (Figure 5b). The pattern differed by cluster where 28% of daily density gradients were significantly related to wind shear stress in rarely mixed sites, 10% in intermittently mixed sites, and 83% in often mixed sites. Convective heat transfer was only related to density gradients in a few sites (7/34) (Figure 5c). When examining by cluster, 11% of daily density gradients were significantly related to convective heat transfer in rarely mixed sites, 50% in intermittently mixed sites, and 0% in often mixed sites. Most of the time series models were simple models with the residuals including only first or second order auto-regressive and, at most, two moving average terms (Table S5 in Supporting Information S1). As the maximum depth increased, the relationship between short wave radiation and density gradient exponentially decreased (Figure 6a,  $\beta = 0.27e^{-0.71 \times \text{max. depth}}$ ,  $df = 32$ ,  $p = 0.037$ ,  $R^2 = 0.19$ ). There was an inverse relationship between waterbody surface area and the density gradient response to wind shear stress, with larger waterbodies more affected by wind (Figure 6b,  $\beta = -0.06 - 0.04 \log(\text{surface area})$ ,  $F_{1,32} = 10.9$ ,  $p = 0.002$ ,  $R^2 = 0.23$ ). There were no other relationships between maximum depth or surface area and other  $\beta$ s.

### 3.4. Precipitation Events

We identified 30 precipitation events across 22 waterbodies where there was a day of minimal precipitation ( $< 25.4 \text{ mm}$ ), followed by a day with  $> 25.4 \text{ mm}$  of precipitation, followed by a day with minimal precipitation. In 77% of the precipitation events, the density gradient showed a decreasing pattern

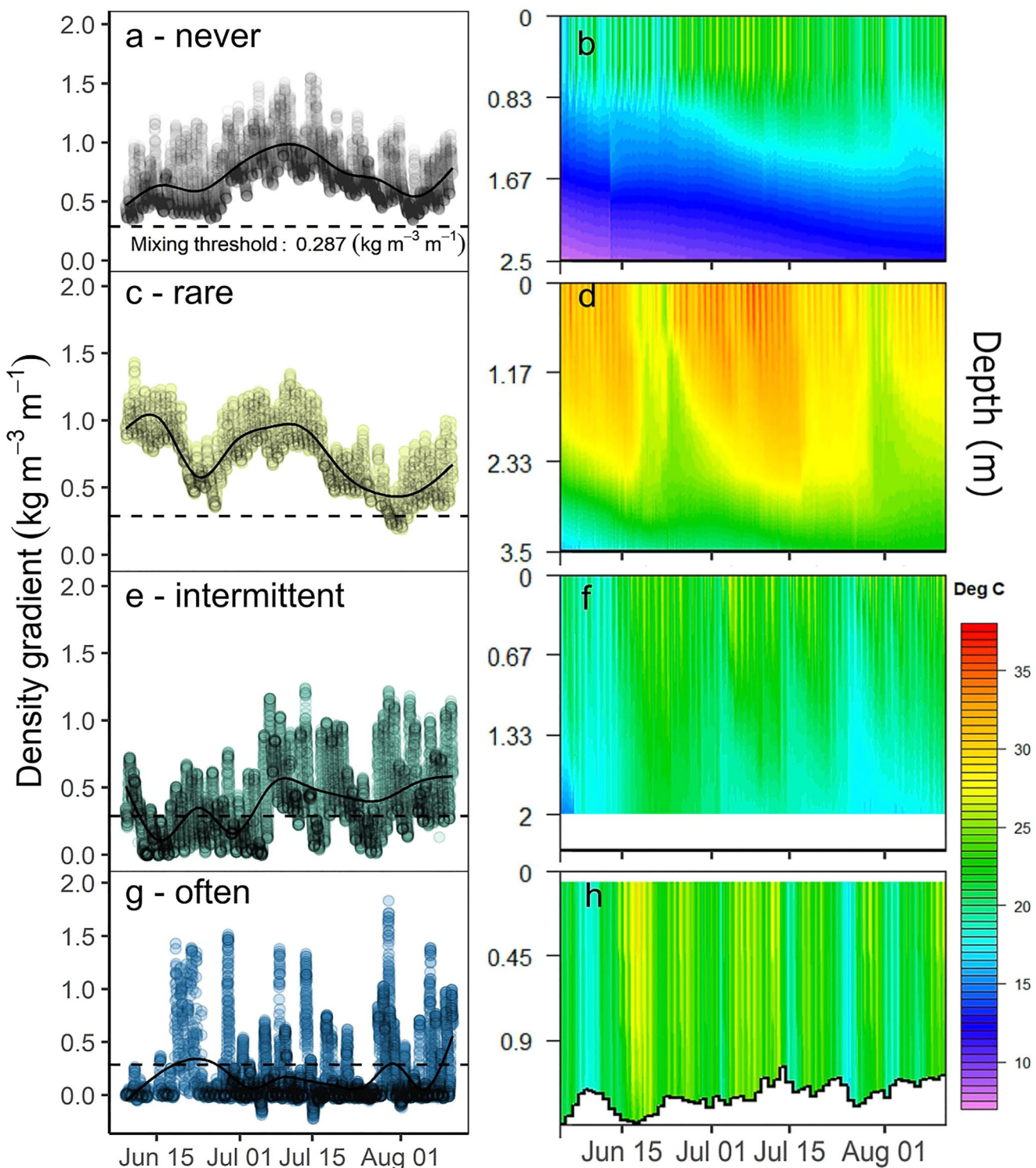


**Figure 2.** Examples of the wide range of mixing patterns observed in shallow waterbodies, from never mixed to often mixed. (a) density gradient for Gibson Pond - never mixed, this category was grouped with rarely mixed but is shown for illustrative purposes, (b) heatmap of Gibson Pond, (c) density gradient for Bethel Lake - rarely mixed, (d) heatmap of Bethel Lake, (e) density gradient for Pond 4A - intermittently mixed, (f) heatmap of Pond 4A, (g) density gradient for Simpson Bay - often mixed, (h) heatmap of Simpson Bay. In the left-hand column, the black solid lines are locally estimated scatterplot smoothing fits and dashed horizontal lines are the  $0.287 \text{ kg m}^{-3} \text{ m}^{-1}$  mixing threshold. In the right-hand column, the black solid line at the bottom of the heat map represents the waterbody's maximum depth, which varied in some sites.

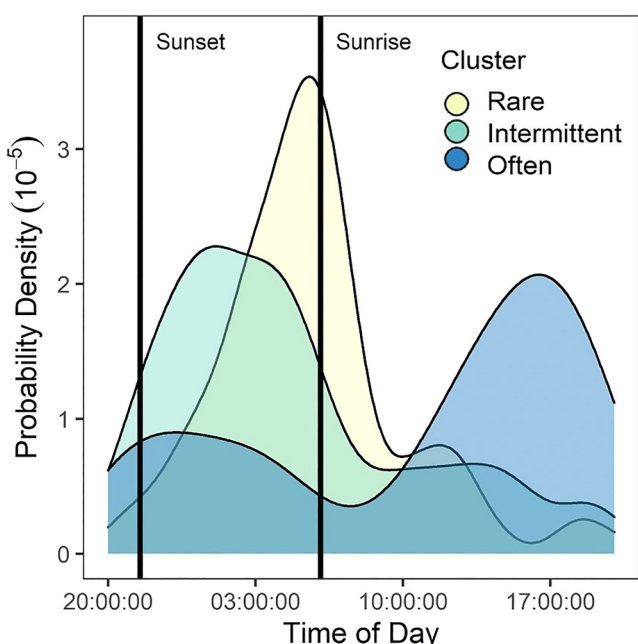


**Figure 3.** Probability density functions showing the time on each day when waterbodies within each cluster dropped below the  $0.287 \text{ kg m}^{-3} \text{ m}^{-1}$  density gradient threshold, signifying mixing. The vertical black lines represent sunset (21:30) and sunrise (06:00) for 10 July at the median latitude from all study sites. Rare = rarely mixed; Intermittent = intermittently mixed; Often = often mixed.

either the day of or day following the precipitation event (Figure 7a). On the day of the precipitation event, five sites exhibited mixing where the density gradient dropped below the  $0.287 \text{ kg m}^{-3} \text{ m}^{-1}$  threshold. Of those five waterbodies with mixing events, four were in the intermittently mixed cluster and one was in the often mixed cluster. For two additional sites, waterbodies had density gradients below the mixing cutoff prior to the precipitation event and stayed mixed throughout the event. When the density gradients were standardized as percentage decrease relative to the day preceding the event, the median density decrease was  $-17.8\%$  on the day of the event and  $-25.8\%$  on the day following the event (Figure 7b). When broken down by cluster, only two precipitation events occurred in often mixed sites (Figure 7c); therefore, we only compared between the rare and intermittent clusters. There were no statistical differences between the decline in percent change in the density gradient on the day of the event ( $\chi^2 = 1.8, p = 0.18, \text{df} = 1$ , Figure 7c) or the day after the event ( $\chi^2 = 0.07, p = 0.79, \text{df} = 1$ , Figure 7c).

In 2019 in southern Minnesota, there were 2 days (28–29 June 2019) with no rain followed by a 2 day event resulting in 56.6 mm of total precipitation (26.4 and 30.2 mm on 30 June 2019 and 01 July 2019, respectively; Figure 8b). We monitored 12 waterbodies in this region, 11 of which were in the rarely mixed cluster and the remaining site (Big Pond) was in the intermittently mixed cluster. Across most of the 12 sites, the density gradient responded quickly to precipitation (Figure 8a). During the intense early morning rain on 30 June, the density gradient between top and bottom waters decreased in all 12 waterbodies. There was a slight rebound during the break in precipitation during the day, followed by another midday rain that interrupted the increasing density gradient. During the large rain event overnight, the density difference continued to drop and remained depressed with delayed and minimal increases the next day. In general, during the 2 days with precipitation, the maximum density gradient was 70% lower compared to the preceding 2 days

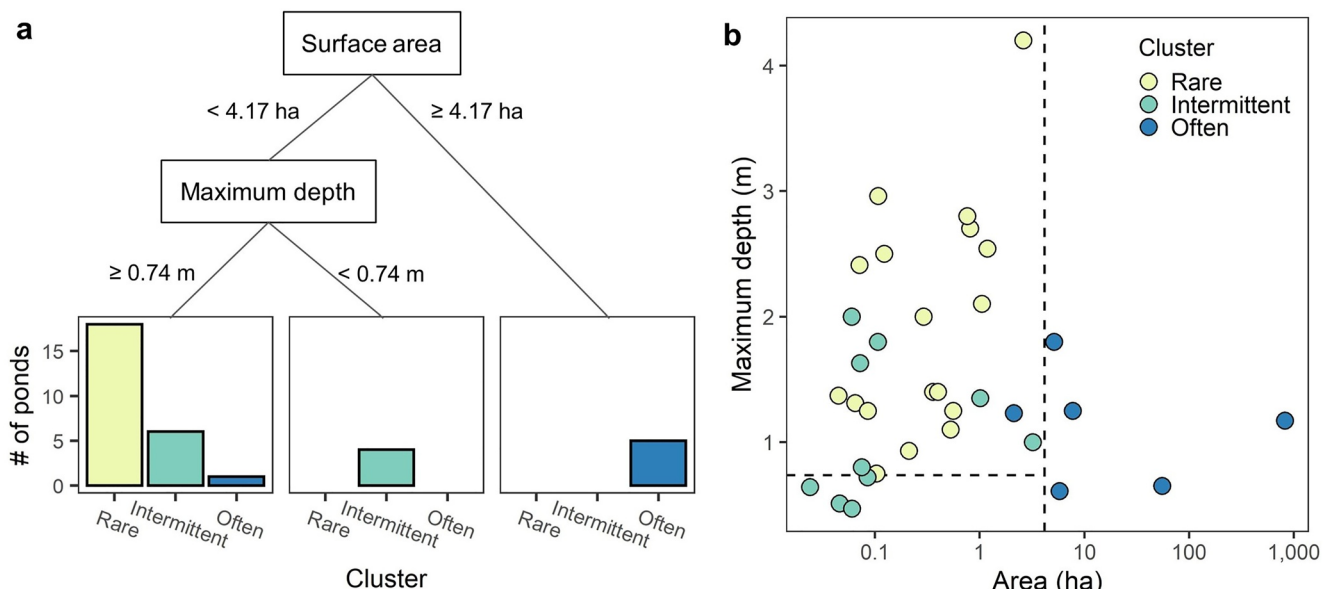


**Figure 4.** Surface area and maximum depth best predicted the probability that the water column will mix during the summer season, which was used to categorize waterbodies into distinct mixing clusters. (a) The classification and regression tree (CART) model identified two splits, first by surface area at  $4.17 \text{ ha}$  and a second split based on maximum depth at  $0.74 \text{ m}$ . Barplots represent the number of sites in each cluster when following the two splits. (b) Biplot of surface area and maximum depth, colored by cluster. Dashed lines indicate locations of CART splits based on surface area and maximum depth. Rare = rarely mixed; Intermittent = intermittently mixed; Often = often mixed.

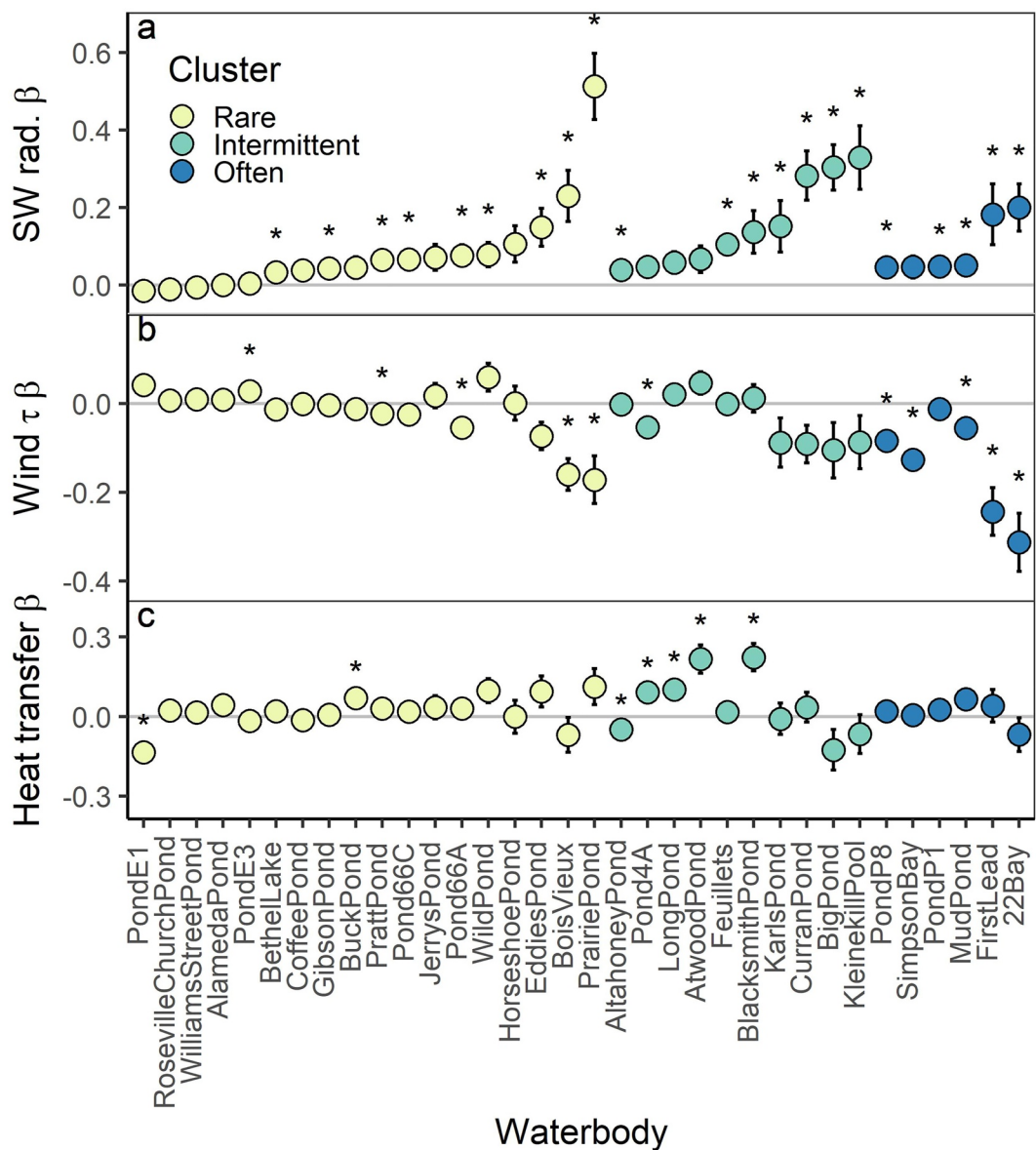


**Figure 5.** Relationship between z-transformed (a) total daily shortwave radiation (SW rad.), (b) maximum wind shear stress (wind  $\tau$ ), and (c) mean convective heat transfer (heat transfer) and the daily mean density gradient for all 34 waterbodies in this study. \* indicates  $\beta$  was significantly different than 0. The waterbodies are ranked by cluster (rare, intermittent, and often mixed) and then by SW radiation  $\beta$ . Error bars are standard errors and may be obscured by the size of the point.

across all 12 waterbodies. Three waterbodies located in close proximity to each other, Roseville Church, William Street, and Alameda, were all urban sites with lower diel amplitudes in density gradients, and did not respond with the same magnitude as the other nine sites (Figure 8a). In the 2 days following the major precipitation events, the maximum density gradients rebounded close to the pre-event days (i.e., 87% of the 2 days preceding the precipitation events). Across the 2 days of precipitation, the only site (Big Pond) to completely mix represented the only site in the intermittently mixed category; this pond remained mixed for most of those 2 days.

#### 4. Discussion

By examining 34 temperate ponds and shallow lakes, our study rejects the long-held assumption that shallow waterbodies are continuously mixed systems. Rather, shallow waterbodies commonly stratify during the summer and can be grouped into one of three mixing regimes: rarely, intermittently, and often mixed, with rare

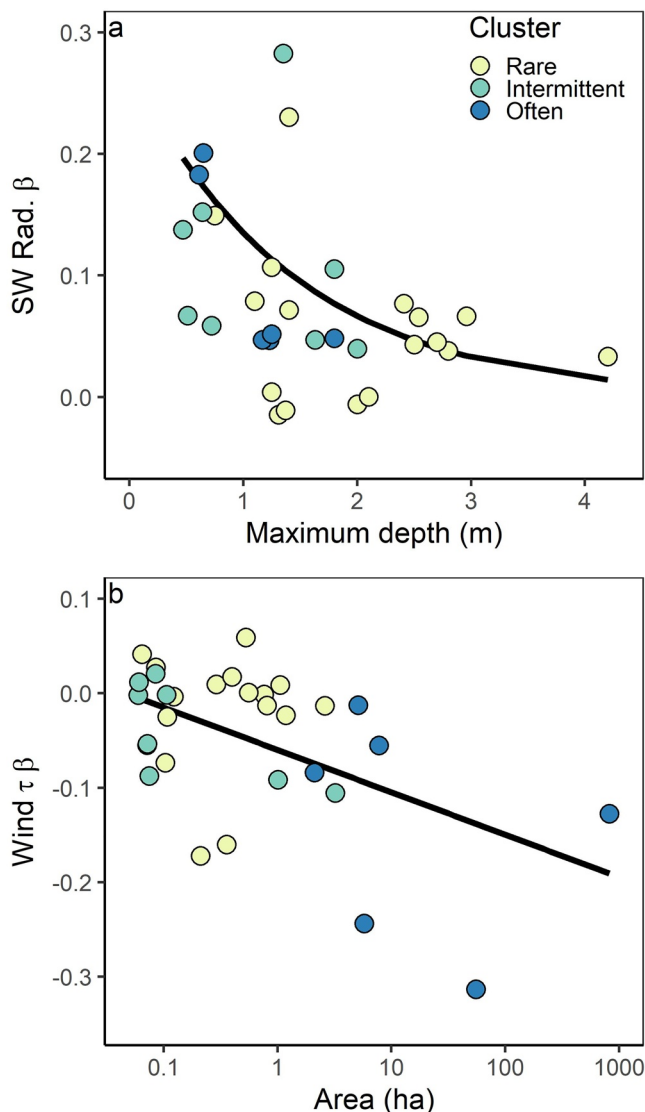


**Figure 6.** (a) Exponential relationship between the short wave radiation (SW Rad.) time series coefficient ( $\beta$  between z-transformed total daily SW Rad. and daily mean density gradient) and maximum depth in each waterbody. (b) Linear relationship between wind shear stress (Wind  $\tau$ ) time series coefficient ( $\beta$  between: z-transformed max daily wind  $\tau$  and daily mean density gradient) and surface area in each waterbody. Sites are colored by mixing cluster (rare, intermittent, and often mixed). Black line indicates least-squares best fit regression line across all clusters.

Water depth further explains pond mixing: shallow ponds  $<0.74$  m mix intermittently whereas deeper ponds mix rarely or never (Figure 4). Less water volume in shallower waters means that thermal dynamics can strongly respond to solar radiation (Figure 6a) and heat transfer (Figure 5c), allowing for convective cooling to mix waters overnight (MacIntyre et al., 2010; Read et al., 2012). The timing of mixing also provides evidence of convective cooling in ponds: rarely and intermittently mixed ponds tended to mix in the morning, compared to afternoon mixing in shallow lakes (Figure 3).

While we identified 0.74 m as a breakpoint between intermittently and rarely mixed sites, ponds 0.74 – 2 m included both rarely- and intermittently- mixing ponds, whereas deeper ponds ( $>2$  m) mixed rarely (Figure 4). Sheltering, pond bathymetry, watershed size, residence time, water transparency, salinity, and groundwater

mixing regimes most prevalent in this study. The three mixing clusters were best predicted by surface area and depth, similar to drivers of mixing and stratification identified in larger lakes (Gorham & Boyce, 1989; Kirillin & Shatwell, 2016; Lathrop & Lillie, 1980). Larger waterbodies ( $\geq 4.17$  ha) mixed often and density gradients responded to solar radiation and wind shear; in smaller waterbodies, stratification was more common and mixing was related to solar radiation and heat transfer. We also found that large precipitation events caused short-term increases in mixing. Identifying distinct mixing regimes in shallow waterbodies is foundational to understanding key ecosystem properties, including oxygen availability, thermal habitats, and nutrient and carbon cycling.

#### 4.1. Three Mixing Regimes and Their Drivers

While small and shallow waterbodies have been assumed to be continuous polymictic (Lewis Jr., 1983; Scheffer, 2004), only six of our 34 study sites were in the often-mixed cluster, which mixed 75% of the time on average (Figure 1c). All six sites were relatively large ( $>2.1$  ha) and shallow ( $<2$  m maximum depth), representative of shallow lakes, which are differentiated from deeper lakes due to greater light penetration, macrophyte cover, nutrient recycling, and mixing (Fairchild et al., 2005; Richardson et al., 2022; Scheffer, 2004). The relatively large fetch and strong wind shear relative to water depth supports a well-mixed water column, even in the summer (Padisák & Reynolds, 2003; Scheffer, 2004; Torremorell et al., 2007). Our analysis supported the importance of wind-driven mixing: wind shear weakened stratification in often-mixed sites (Figure 5b), with the strongest effects in larger waterbodies (Figure 6b). Additionally, often-mixed sites tended to mix mid-afternoon (Figure 3) when wind speeds are strongest (Dai & Deser, 1999). While continuous mixing waterbodies were rare in our data set, they are likely common in regions with abundant shallow lakes, such as the tropics and subtropics (e.g., Pampean lakes in Argentina; Dióvisalvi et al., 2015) or the circumpolar Arctic (Rautio et al., 2011).

While shallow lakes are described to range in surface area from less than a hectare to over 100 km<sup>2</sup> (Scheffer, 2004), we found that mixing regimes differed across the size gradient and may help functionally distinguish ponds from shallow lakes (Fairchild et al., 2005). Specifically, we identified a size threshold of 4.17 ha between continuously mixed shallow lakes (i.e., “often mixed” cluster) and discontinuously mixed ponds (i.e., “intermittently mixed” and “rarely mixed” clusters), which stratified for days to weeks at a time (Figure 4). Reduced mixing in ponds can be explained by a smaller fetch and greater sheltering from surrounding vegetation and topography that dampen wind-generated turbulence (Markfort et al., 2010). With reduced wind shear and smaller volume, ponds respond strongly to solar radiation (Figure 5a) and can heat up dramatically during the day, inducing stratification.

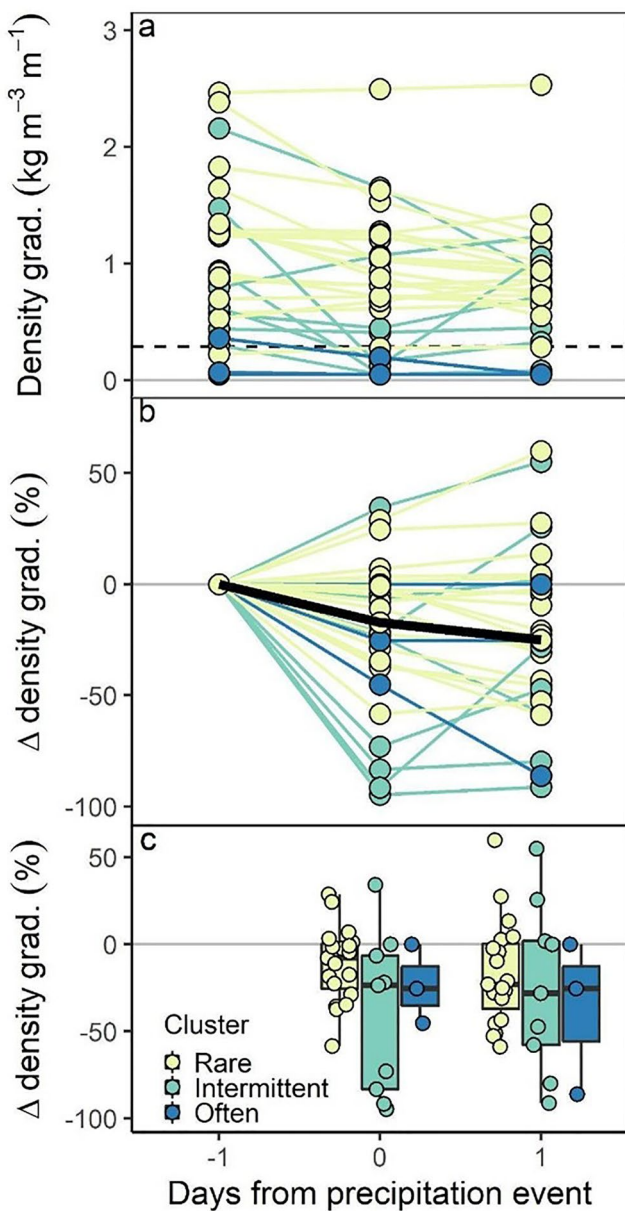


**Figure 7.** All precipitation events with  $>25.4 \text{ mm}$  precipitation in a single day with the day prior to the event (day = -1), day of the event (day = 0), and day after the event (day = 1) for waterbodies compared across (a) the mean daily density gradient, (b) percent change in density gradient from the day before the event with the black line representing the average change across sites, and (c) the percent change relative to the day before the event broken down by cluster. Boxplots represent the median  $\pm$  interquartile range with whiskers extending to 5th and 95th percentiles. Rare = rarely mixed; Intermittent = intermittently mixed; Often = often mixed.

et al., 2021), ponds may have a greater response as they take less energy to mix. In addition to precipitation, storms could also reduce stratification strength through drops in air temperature, reduced solar radiation, and increases in wind speed (Jennings et al., 2012; Song et al., 2013).

We observed a macrosystem response where 12 waterbodies within one region responded similarly to a single storm (Figure 8). Heavy precipitation weakened stratification in 11 rarely mixed ponds, with no noticeable

inputs could all potentially shift the mixing regime in these intermediately deep ponds (e.g., Winslow et al., 2015). Future research should explore this mixing regime transition (0.74 – 2 m), especially the role of sheltering as ponds in open landscapes may mix more easily than ponds surrounded by forest or riparian vegetation. Ultimately, depth differences of less than a few meters can dramatically change pond mixing regimes, explaining why similarly sized ponds ( $<0.5 \text{ ha}$ ) can mix nightly or weekly if shallow ( $<1 \text{ m}$ ; Andersen et al., 2017; Branco & Torgersen, 2009; Holgerson et al., 2016), or can stratify for much of the summer if deeper (e.g., 4 m; Moss, 1969).

Besides surface area and depth, no other pond characteristics predicted the three mixing clusters and few characteristics differed among the mixing clusters (Table S4, Figure S7 in Supporting Information S1). We expected reduced mixing with increased  $K_D$  due to greater chlorophyll *a*, DOC, and vegetative cover. Previous studies found that increased DOC reduced mixing in a small (3 ha) and shallow ( $<3 \text{ m}$ ) lake (Brothers et al., 2014), and increased phytoplankton could reduce water transparency, increase stratification, and induce mixing regime shifts in lakes 5 – 8 m deep (Shatwell et al., 2016). Vegetative cover, particularly by submerged macrophytes, can also strengthen stratification by physically blocking light to the benthos, dissipating kinetic energy, and converting radiant energy to heat to warm the water above the macrophytes (Chimney et al., 2006; Herb & Stefan, 2004; Sand-Jensen et al., 2019). It is possible that the impact of altered light attenuation on mixing is more evident when comparing changes within a single waterbody, where depth and area are constant. The lack of relationship between mixing and submerged vegetation may also relate to the positive correlation between fetch and submerged cover ( $r = 0.44$ , Table S3 in Supporting Information S1) as high wind speeds may negate the stabilizing role of submerged macrophytes. Future studies could use whole-pond experiments to examine the interaction of light attenuation and macrophytes on mixing regime.

#### 4.2. Meteorological Impacts on Mixing

Overall, solar radiation increased density gradients across all waterbodies, with the strongest responses in the shallowest waterbodies, whereas wind shear broke down stratification, with the strongest responses in the biggest waterbodies (Figure 5). The different responses relate to waterbody morphometry, as turbulent mixing is dominated by wind shear in large waterbodies and by convective cooling in small waterbodies (Read et al., 2012). Daily precipitation did not directly link to density gradients (data not shown) because there were many days with no or small amounts of precipitation. However, moderate to large precipitation events reduced the magnitude of stratification substantially and, in some cases, mixed the ponds (Figures 7 and 8). One mechanism for this could come from the direct contribution of colder water to the pond. For example, 25.4 mm of precipitation would directly increase volume of our study ponds by 1.4%–8.4% depending on pond depth, but only represent an additional 0.4% of volume in a larger lake with a mean depth of 7 m. Consequently, while water temperatures in lakes may not respond to small precipitation events (Andersen et al., 2020; Doubek

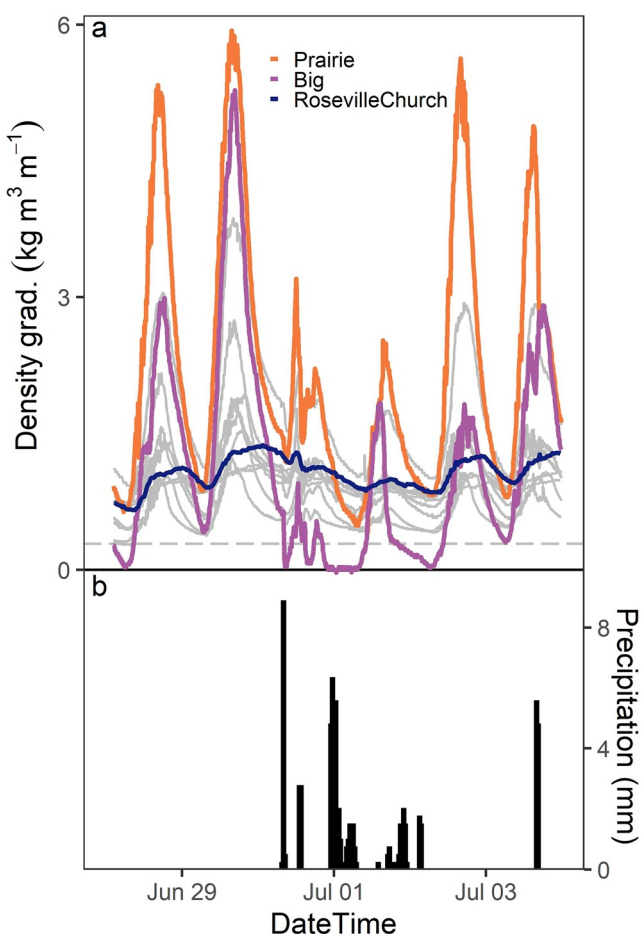


**Figure 8.** (a) Density gradient of 12 waterbodies from southeastern Minnesota during a 6 day period from 28 June 2019 to 03 July 2019 with (b) 56.6 mm precipitation occurring on 30 June and 01 July (and 70.4 mm total precipitation across all 6 days). Three sites are highlighted in color including Prairie Pond (peak density gradient), Big Pond (dropped below the mixing threshold indicated by dashed line), and Roseville Church Pond (one of three with low amplitudes prior to the precipitation event); the remaining nine are in gray behind. Precipitation totals were collected at the most central location and were similar across all 12 waterbodies (range in 2 day precipitation total: 39.2–56.6 mm).

changes to wind speed. The one intermittently mixed pond in this region mixed completely during the storm, also likely driven by precipitation although wind speeds did increase at this site for a few hours during the storm. Our observation of a few days of rain is much smaller in scope but analogous to extreme events like tropical cyclones that can weaken or disrupt summer stratification of multiple lakes and reservoirs across broad scales (Klug et al., 2012; Woolway et al., 2018). For these smaller precipitation events, the responses occur at a sub-daily temporal scale where there is a quick response to the precipitation followed by a return to diel trends (Figure 8; Andersen et al., 2020; Woolway et al., 2018). The response of waterbodies' mixing regime to meteorological variables is especially important in the context of the rapidly changing climate. For example, stratification will likely get stronger due to both warmer air temperatures (Oleksy & Richardson, 2021) and atmospheric stilling (Woolway et al., 2017), whereas more intense storm events may simultaneously increase the frequency of complete mixing events in ponds.

#### 4.3. Defining Mixing Using Density Thresholds

Temperature or density differences, density gradients, and turbulence measurements have all been used to define mixing in lentic ecosystems (reviewed in Gray et al., 2020). Using density is preferable due to the non-linear relationship between water temperature and density, and because water density differences directly establish strata. Similarly, other metrics like the relative thermal resistance to mixing or Schmidt stability have been used to identify thermal stratification (e.g., Oleksy & Richardson, 2021; Siver et al., 2018). However, the choice of a density gradient, density difference, or other stratification metric thresholds have been arbitrary or based on subjective visual assessments (e.g., Giling, Staehr, et al., 2017; Staehr et al., 2012) and could have implications for weakly stratified or polymictic systems. In this study, pond clusters were relatively insensitive to the range of density gradient cutoffs from literature (Gray et al., 2020) with most ponds fitting stably into one cluster (Table S2 in Supporting Information S1). However, the proportion of time that an often mixed pond was considered mixed changed with the density gradient threshold. For example, as the density threshold increased, the proportion of time a pond was mixed during the day doubled in the often mixed cluster (Figures 1a–1d), with less dramatic changes at night and in the other two clusters. We concur with Gray et al. (2020) that it is valuable to consider a range of density thresholds when quantifying mixing.

For future studies, calculations of heat budgets and additional stratification parameters would be valuable, particularly comparing water friction velocity ( $u^*$ , units:  $\text{m s}^{-1}$ ) and waterside velocity for convection ( $w^*$ ) to differentiate between wind shear and convection (Imberger, 1985). However, the underlying assumptions for these calculations were derived for lakes and may not scale to smaller waterbodies. For example, we used 10 m wind speeds to calculate wind shear stress in this study and  $u^*$  is scaled to wind speeds 10 m above the water surface (e.g., Read et al., 2011). However, typical boundary layer scaling of wind speed (e.g., Amorosco & DeVries, 1980) may be unrealistic in ponds where small fetch and sheltering could prohibit boundary layers from forming the same way as they do in lakes (Markfort et al., 2010; Vesala et al., 2006). Therefore, evaluating the wind shear stress that ponds experience will require measurements of sheltering by surrounding vegetation (i.e., trees, emergent macrophytes) and wind measurements in the middle of the pond. Additionally,  $w^*$  and other lake mixing metrics (e.g., lake number and Wedderburn number) require estimating exact thermocline depths or metalimnion boundaries, which may be at scales smaller than the thermistor sensor resolution deployed in most studies. These challenges will be important to address when applying lake stratification metrics to small or shallow waterbodies.

#### 4.4. Implications for Ecological and Biogeochemical Processes

Different mixing regimes likely impact key ecosystem processes, including oxygen availability, nutrient recycling, ecosystem metabolism, and greenhouse gas production and emissions. For example, often mixed shallow lakes may have high oxygen availability throughout the water column, whereas smaller ponds may have hypoxic or anoxic bottom waters during periods of stratification. Hypoxic waters can be energetically expensive and even limit survival for many organisms, including fish, amphibians, and invertebrates (Saari et al., 2018). Hypoxic waters also have higher concentrations of redox-sensitive nutrients and contaminants, which can be brought to the surface during short-term mixing events (Barrett et al., 2018; Taguchi et al., 2020; Wilhelm & Adrian, 2007). For instance, short-term mixing events can increase surface water nutrient concentrations and promote phytoplankton or cyanobacteria blooms (Giling, Nejstgaard, et al., 2017; Wilhelm & Adrian, 2007) and even elevate gross primary production for weeks after mixing (Giling, Nejstgaard, et al., 2017). Similarly, mixing regimes can affect greenhouse gas production and emissions. Anoxic bottom waters promote methane ( $\text{CH}_4$ ) production, which can be released to the atmosphere if a waterbody mixes quickly (Erkkilä et al., 2018; Vachon et al., 2019). As such, carbon emissions may increase when ponds mix overnight, a phenomenon seen in a large shallow lake (Podgrajsek et al., 2014) and a boreal fen (Godwin et al., 2013). A corollary is that stratification may reduce emissions, as seen in farm ponds that consume nitrous oxide (Webb et al., 2019). Mixing regime may also influence the balance of carbon storage versus emissions as increased stratification can promote carbon burial in lakes through cooler bottom water (Bartosiewicz et al., 2019) and anoxia (Carey et al., 2022). As mixing regimes may regulate ecology and biogeochemistry, monitoring mixing patterns may be necessary to predict greenhouse gas budgets and accurately model ecosystem dynamics.

#### 4.5. Conclusion: An Updated Paradigm on Mixing in Small, Shallow Waterbodies

We identified that small, shallow waterbodies have a variety of mixing regimes, and can no longer be assumed to be continuously polymictic. Rather, we propose a new paradigm where temperate shallow waterbodies have three mixing regimes (Figure 9), which are likely functionally distinct in ecological and biogeochemical processes (Fairchild et al., 2005; Richardson et al., 2022). First, larger shallow lakes that continuously mix are distinguished from smaller ponds that commonly stratify. Second, discontinuously mixed ponds can be split into shallow ponds that mix intermittently versus deeper ponds that mix rarely. The exact size and depth transitions among catego-

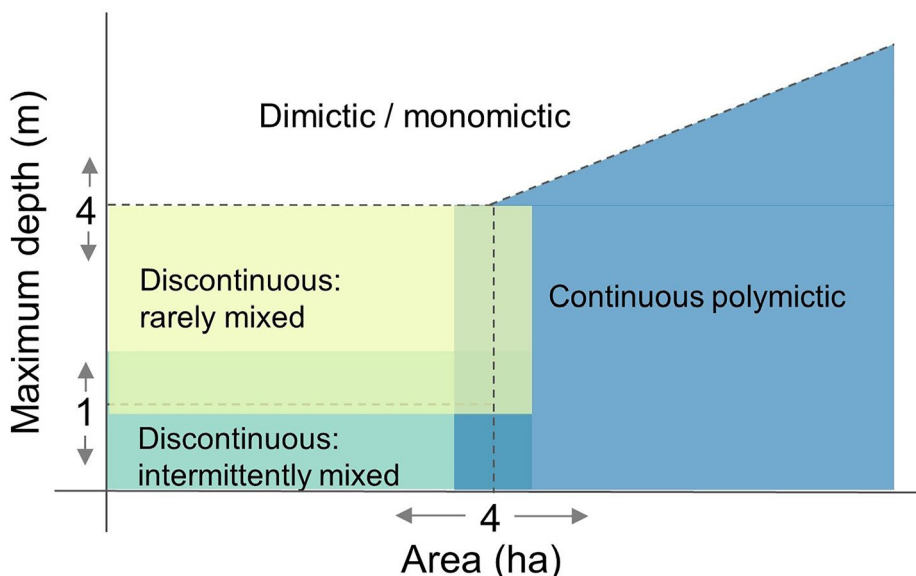


**Figure 9.** Proposed paradigm of mixing in small and shallow waterbodies in temperate regions. Small ( $<\sim 4$  ha) and shallow ( $<\sim 4$  m) ponds mix discontinuously, with intermittent mixing in shallower compared to deeper ponds, which rarely mix. In larger, shallow waterbodies (i.e., shallow lakes), continuous mixing occurs. The exact boundaries (dashed lines) among categories depend on fetch, sheltering, and transparency, and need further resolution. In particular, this study did not address the upper boundaries between polymictic and dimictic/monomictic systems (see text).

## Acknowledgments

This project emerged during a brainstorming session at the Global Lake Ecological Observatory Network (GLEON) 19 meeting at Mohonk Lake, New York, when the Pond Observation aNd Discovery in GLEON (PONDING) group formed. We thank all municipalities and landowners who granted us access to study sites, including the Katharine Ordway Natural History Study Area of Macalester College, the St. Olaf College Natural Lands, Mohonk Preserve, Minnewaska State Park Preserve, Curran Homestead, and the Service de la Biodiversité of the Canton of Geneva. We acknowledge funding support from the St. Olaf College Collaborative Undergraduate Research and Inquiry program (MAH), St. Olaf College Helterbrand/Varshavsky Center for Integrated Research (MAH, JR, KG, and AN), Macalester College Collaborative Summer Research Program (SH), the BEYOND 2020 project funded under the Marine Research Programme by the Irish Government (grant PBA/FS/16/02, MRA), the Minnesota Stormwater Research and Technology Transfer Program via the University of Minnesota Water Resources Center and the Minnesota Stormwater Research Council (JCF and BDI), the MANTEL ITN through the European Union's Horizon 2020 Research and Innovation Programme under the Marie Skłodowska-Curie (grant 722518, JPM), the University of Missouri School of Natural Resources (RLN), the North Central Region Water Network (grant 0057039, RLN), National Science Foundation: 1559769 (to Alan Berkowitz, funding COR), Ducks Unlimited Canada (LEB), the Saskatchewan Ministry of Agriculture's Agricultural Development Fund (grant 20160015, KF and JRW) and the Great Plains Cooperative Ecosystems Study Unit (grant G16AC00003, JNS). Any use of trade, firm, or product names is for descriptive purposes only and does not imply endorsement by the U.S. Government. We are grateful to the following people for assistance during field work: Eliane Demierre, Lianna Goldstein, Margot Groskreutz, Kathryn Hoffman, Sarah Hoffman, Kui Hu, Sydney Jensen, Olivia Johnson, Emily Kinzinger, Paige Kowal, Ally Kruper, Jacob Meier, Megan Napoli, Beat Oertli, Jean Pengra, and Jillian St. George. We thank Alana Barnhart for assistance with data cleaning and preliminary analyses. We appreciate the thoughtful reviews by Hilary Dugan and anonymous reviewers, which improved this manuscript. We acknowledge, with respect, that the study ponds in North America are located on the homelands of Indigenous peoples including the Anishinaabe, Anishnápek, Lenape, Métis, Nipmuc, Néhiyawak, Očeti Sakowin, Osage, Penobscot, and Peoria. We make this acknowledgment to honor all Indigenous people, ancestors, and descendants, as well as the land itself.

ries need further resolution, and may respond to other variables such as sheltering and water transparency. For instance, increased sheltering or decreased transparency would trap more heat in the surface waters and increase stratification (Kirillin & Shatwell, 2016). Mixing regimes in shallow waterbodies may also differ outside of temperate regions; for example, high latitude systems potentially mix more often due to cooler temperatures especially in more open landscapes.

Our study did not specifically evaluate the upper boundary between polymictic and dimictic/monomictic systems. We propose 4 m as the maximum depth transition, which was informed by the depth cutoff for shallow lakes (3–5 m; Padisák & Reynolds, 2003; Richardson et al., 2022; Scheffer, 2004) and the location where the size-depth relationship may break down in lakes (4 m; Lathrop & Lillie, 1980). The transition between polymictic and dimictic is particularly relevant for eight ponds in the discontinuous rarely mixed cluster that were always stratified during our study. Determining whether their mixing regime is discontinuous or dimictic requires examining the spring and fall shoulder seasons as well as ice cover; for example, 120 days of stratification has been proposed as a cutoff between polymictic and dimictic lakes (Kirillin & Shatwell, 2016). Ultimately, this updated paradigm (Figure 9) captures the prevalence of stratification and variability of mixing regimes in ponds and shallow lakes, which impact key ecosystem processes.

## Data Availability Statement

Data are archived in a Dryad data repository <https://datadryad.org/stash/share/sifvTmDNSjf7RrkzEZIAQLjGzuYv6tGW409JC38V1g>, available here: <https://10.5061/dryad.t4b8gtj4q>. Data from Ponds E1 and E3 can also be found in Bansal et al. (2020) and data from Bethel Lake found in Kinzinger and North (2021).

## References

Amoroch, J., & DeVries, J. J. (1980). A new evaluation of the wind stress coefficient over water surfaces. *Journal of Geophysical Research*, 85(C1), 433–442. <https://doi.org/10.1029/JC085iC01p00433>

Andersen, M. R., de Eyt, E., Dillane, M., Poole, R., & Jennings, E. (2020). 13 years of storms: An analysis of the effects of storms on lake physics on the Atlantic fringe of Europe. *Water*, 12(2), 318. <https://doi.org/10.3390/w12020318>

Andersen, M. R., Krugh, T., Martinsen, K. T., Kristensen, E., & Sand-Jensen, K. (2019). The carbon pump supports high primary production in a shallow lake. *Aquatic Sciences*, 81(2), 24. <https://doi.org/10.1007/s00027-019-0622-7>

Andersen, M. R., Sand-Jensen, K., Iestyn Woolway, R., & Jones, I. D. (2017). Profound daily vertical stratification and mixing in a small, shallow, wind-exposed lake with submerged macrophytes. *Aquatic Sciences*, 79(2), 395–406. <https://doi.org/10.1007/s00027-016-0505-0>

Bansal, S., Meier, J. A., & Tangen, B. A. (2020). *Temperature and light measurements along the water-depth profile of ponds in North Dakota, USA*, 2019. U.S. Geological Survey Data Release. <https://doi.org/10.5066/P9ZFX7KQ>

Barrett, P. M., Hull, E. A., King, C. E., Burkart, K., Ott, K. A., Ryan, J. N., et al. (2018). Increased exposure of plankton to arsenic in contaminated weakly-stratified lakes. *Science of the Total Environment*, 625, 1606–1614. <https://doi.org/10.1016/j.scitotenv.2017.12.336>

Bartosiewicz, M., Przytulska, A., Lapierre, J., Laurion, I., Lehmann, M. F., & Maranger, R. (2019). Hot tops, cold bottoms: Synergistic climate warming and shielding effects increase carbon burial in lakes. *Limnology and Oceanography Letters*, 4(5), 132–144. <https://doi.org/10.1002/lol2.10117>

Biggs, J., Williams, P., Whitfield, M., Nicolet, P., & Weatherby, A. (2005). 15 years of pond assessment in Britain: Results and lessons learned from the work of pond conservation. *Aquatic Conservation: Marine and Freshwater Ecosystems*, 15(6), 693–714. <https://doi.org/10.1002/aqc.745>

Branco, B. F., & Torgersen, T. (2009). Predicting the onset of thermal stratification in shallow inland waterbodies. *Aquatic Sciences*, 71(1), 65–79. <https://doi.org/10.1007/s00027-009-8063-3>

Brothers, S., Köhler, J., Attermeyer, K., Grossart, H. P., Mehner, T., Meyer, N., et al. (2014). A feedback loop links brownification and anoxia in a temperate, shallow lake. *Limnology & Oceanography*, 59(4), 1388–1398. <https://doi.org/10.4319/lo.2014.59.4.1388>

Bukaveckas, P. A., & Driscoll, C. T. (1991). Effects of whole-lake base addition on thermal stratification in three acidic Adirondack lakes. *Water, Air, and Soil Pollution*, 59(1–2), 23–39. <https://doi.org/10.1007/BF00283170>

Carey, C. C., Hanson, P. C., Thomas, R. Q., Gerling, A. B., Hounshell, A. G., Lewis, A. S. L., et al. (2022). Anoxia decreases the magnitude of the carbon, nitrogen, and phosphorus sink in freshwater. *Global Change Biology*, 16228. <https://doi.org/10.1111/gcb.16228>

Chang, W., Cheng, J., Allaire, J. J., Sievert, C., Schloerke, B., Xie, Y., et al. (2021). shiny: Web application framework for R (Version 1.6.0). Retrieved from <https://CRAN.R-project.org/package=shiny>

Chimney, M. J., Wenkert, L., & Pietro, K. C. (2006). Patterns of vertical stratification in a subtropical constructed wetland in south Florida (USA). *Ecological Engineering*, 27(4), 322–330. <https://doi.org/10.1016/j.ecoleng.2006.05.017>

Choffel, Q., Touchart, L., Bartout, P., & Al Domany, M. (2017). Temporal and spatial variations in heat content of a French pond. *Geographia Technica*, 12(1), 9–22. [https://doi.org/10.21163/GT\\_2017.121.02](https://doi.org/10.21163/GT_2017.121.02)

Dai, A., & Deser, C. (1999). Diurnal and semidiurnal variations in global surface wind and divergence fields. *Journal of Geophysical Research*, 104(D24), 31109–31125. <https://doi.org/10.1029/1999JD900927>

Diovisalvi, N., Bohn, V. Y., Piccolo, M. C., Perillo, G. M. E., Baigún, C., & Zagarese, H. E. (2015). Shallow lakes from the central Plains of Argentina: An overview and worldwide comparative analysis of their basic limnological features. *Hydrobiologia*, 752(1), 5–20. <https://doi.org/10.1007/s10750-014-1946-x>

Doubek, J. P., Anneville, O., Dur, G., Lewandowska, A. M., Patil, V. P., Rusak, J. A., et al. (2021). The extent and variability of storm-induced temperature changes in lakes measured with long-term and high-frequency data. *Limnology & Oceanography*, 66(5), 1979–1992. <https://doi.org/10.1002/lno.11739>

Downing, J. (2010). Emerging global role of small lakes and ponds: Little things mean a lot. *Limnética*, 29(1), 9–24. <https://doi.org/10.23818/limn.29.02>

Erkkilä, K.-M., Ojala, A., Bastviken, D., Biermann, T., Heiskanen, J. J., Lindroth, A., et al. (2018). Methane and carbon dioxide fluxes over a lake: Comparison between eddy covariance, floating chambers and boundary layer method. *Biogeosciences*, 15(2), 429–445. <https://doi.org/10.5194/bg-15-429-2018>

Fairchild, G. W., Anderson, J. N., & Velinsky, D. J. (2005). The trophic state ‘chain of relationships’ in ponds: Does size matter? *Hydrobiologia*, 539(1), 35–46. <https://doi.org/10.1007/s10750-004-3083-4>

Fee, E. J., Hecky, R. E., Kasian, S. E. M., & Cruikshank, D. R. (1996). Effects of lake size, water clarity, and climatic variability on mixing depths in Canadian Shield lakes. *Limnology & Oceanography*, 41(5), 912–920. <https://doi.org/10.4319/lo.1996.41.5.0912>

Giling, D. P., Nejstgaard, J. C., Berger, S. A., Grossart, H., Kirillin, G., Penske, A., et al. (2017). Thermocline deepening boosts ecosystem metabolism: Evidence from a large-scale lake enclosure experiment simulating a summer storm. *Global Change Biology*, 23(4), 1448–1462. <https://doi.org/10.1111/gcb.13512>

Giling, D. P., Staehr, P. A., Grossart, H. P., Andersen, M. R., Boehr, B., Escot, C., et al. (2017). Delving deeper: Metabolic processes in the metal-minion of stratified lakes: Metalimnetic metabolism in lakes. *Limnology & Oceanography*, 62(3), 1288–1306. <https://doi.org/10.1002/ln.10504>

Godwin, C. M., McNamara, P. J., & Markfort, C. D. (2013). Evening methane emission pulses from a boreal wetland correspond to convective mixing in hollows. *Journal of Geophysical Research: Biogeosciences*, 118, 994–1005. <https://doi.org/10.1002/jgrg.20082>

Gorham, E., & Boyce, F. M. (1989). Influence of lake surface area and depth upon thermal stratification and the depth of the summer thermocline. *Journal of Great Lakes Research*, 15(2), 233–245. [https://doi.org/10.1016/S0380-1330\(89\)71479-9](https://doi.org/10.1016/S0380-1330(89)71479-9)

Gray, E., Mackay, E. B., Elliott, J. A., Folkard, A. M., & Jones, I. D. (2020). Wide-spread inconsistency in estimation of lake mixed depth impacts interpretation of limnological processes. *Water Research*, 168, 115136. <https://doi.org/10.1016/j.watres.2019.115136>

Herb, W. R., & Stefan, H. G. (2004). Temperature stratification and mixing dynamics in a shallow lake with submersed macrophytes. *Lake and Reservoir Management*, 20(4), 296–308. <https://doi.org/10.1080/07438140409354159>

Hocking, G. C., & Straskraba, M. (1999). The effect of light extinction on thermal stratification in reservoirs and lakes. *Internationale Revue Der Gesamten Hydrobiologie Und Hydrographie*, 84, 535–556. <https://doi.org/10.1002/iroh.199900046>

Holgerson, M. A. (2015). Drivers of carbon dioxide and methane supersaturation in small, temporary ponds. *Biogeochemistry*, 124(1–3), 305–318. <https://doi.org/10.1007/s10533-015-0099-y>

Holgerson, M. A., & Raymond, P. A. (2016). Large contribution to inland water CO<sub>2</sub> and CH<sub>4</sub> emissions from very small ponds. *Nature Geoscience*, 9(3), 222–226. <https://doi.org/10.1038/ngeo2654>

Holgerson, M. A., Zappa, C. J., & Raymond, P. A. (2016). Substantial overnight reaeration by convective cooling discovered in pond ecosystems. *Geophysical Research Letters*, 43(15), 8044–8051. <https://doi.org/10.1002/2016GL070206>

Hutchinson, G. E., & Loeffler, H. (1956). The thermal classification of lakes. *Proceedings of the National Academy of Sciences*, 42(2), 84–86. <https://doi.org/10.1073/pnas.42.2.84>

Hyndman, R., Athanasopoulos, G., Bergmeir, C., Caceres, G., Chhay, L., O’Hara-Wild, M., et al. (2021). forecast: Forecasting functions for time series and linear models (Version 8.14). Retrieved from <https://CRAN.R-project.org/package=forecast>

Imberger, J. (1985). The diurnal mixed layer1: The diurnal mixed layer. *Limnology & Oceanography*, 30(4), 737–770. <https://doi.org/10.4319/lo.1985.30.4.0737>

Jennings, E., Jones, S., Arvola, L., Staehr, P. A., Gaiser, E., Jones, I. D., et al. (2012). Effects of weather-related episodic events in lakes: An analysis based on high-frequency data: Episodic events in lakes. *Freshwater Biology*, 57(3), 589–601. <https://doi.org/10.1111/j.1365-2427.2011.02729.x>

Kasprzak, P., Shatwell, T., Gessner, M. O., Gonsiorczyk, T., Kirillin, G., Selmeczy, G., et al. (2017). Extreme weather event triggers cascade towards extreme turbidity in a clear-water lake. *Ecosystems*, 20(8), 1407–1420. <https://doi.org/10.1007/s10021-017-0121-4>

Kinzinger, E. C., & North, R. L. (2021). *Water quality data from Bethel and Stephens Lakes*. 2017–2019. Environmental Data Initiative. <https://doi.org/10.6073/pasta/5f293e04e78922879fca5932ddc54f>

Kirillin, G., & Shatwell, T. (2016). Generalized scaling of seasonal thermal stratification in lakes. *Earth-Science Reviews*, 161, 179–190. <https://doi.org/10.1016/j.earscirev.2016.08.008>

Klug, J. L., Richardson, D. C., Ewing, H. A., Hargreaves, B. R., Samal, N. R., Vachon, D., et al. (2012). Ecosystem effects of a tropical cyclone on a network of lakes in northeastern North America. *Environmental Science & Technology*, 46(21), 11693–11701. <https://doi.org/10.1021/es302063v>

Ladwig, R., Rock, L. A., & Dugan, H. A. (2021). Impact of salinization on lake stratification and spring mixing. *Limnology and Oceanography Letters*. <https://doi.org/10.1002/lol2.10215>

Lathrop, R. C., & Lillie, R. A. (1980). Thermal stratification of Wisconsin lakes. *Wisconsin Academy of Sciences, Arts, and Letters*, 68, 90–96.

Lewis, W. M., Jr. (1983). A revised classification of lakes based on mixing. *Canadian Journal of Fisheries and Aquatic Sciences*, 40(10), 1779–1787. <https://doi.org/10.1139/f83-207>

Long, M. H., Rheuban, J. E., Berg, P., & Zieman, J. C. (2012). A comparison and correction of light intensity loggers to photosynthetically active radiation sensors. *Limnology and Oceanography: Methods*, 10(6), 416–424. <https://doi.org/10.4319/lom.2012.10.416>

MacIntyre, S., Jonsson, A., Jansson, M., Aberg, J., Turney, D. E., & Miller, S. D. (2010). Buoyancy flux, turbulence, and the gas transfer coefficient in a stratified lake. *Geophysical Research Letters*, 37(24), L24604. <https://doi.org/10.1029/2010GL04164>

MacIntyre, S., & Melack, J. M. (2010). Mixing dynamics in lakes across climatic zones. In G. Likens (Ed.), *Lake ecosystem ecology: A global perspective*, 86–95. Academic Press.

Magee, M. R., & Wu, C. H. (2017). Response of water temperatures and stratification to changing climate in three lakes with different morphology. *Hydrology and Earth System Sciences*, 21(12), 6253–6274. <https://doi.org/10.5194/hess-21-6253-2017>

Markfort, C. D., Perez, A. L. S., Thill, J. W., Jaster, D. A., Porté-Agel, F., & Stefan, H. G. (2010). Wind sheltering of a lake by a tree canopy or bluff topography. *Water Resources Research*, 46(3). <https://doi.org/10.1029/2009WR007759>

Martinsen, K. T., Andersen, M. R., & Sand-Jensen, K. (2019). Water temperature dynamics and the prevalence of daytime stratification in small temperate shallow lakes. *Hydrobiologia*, 826(1), 247–262. <https://doi.org/10.1007/s10750-018-3737-2>

Mazumder, A., & Taylor, W. D. (1994). Thermal structure of lakes varying in size and water clarity. *Limnology & Oceanography*, 39(4), 968–976. <https://doi.org/10.4319/lo.1994.39.4.0968>

Mesman, J. P., Stelzer, J. A. A., Dakos, V., Goyette, S., Jones, I. D., Kasparian, J., et al. (2021). The role of internal feedbacks in shifting deep lake mixing regimes under a warming climate. *Freshwater Biology*, 66(6), 1021–1035. <https://doi.org/10.1111/fwb.13704>

Moss, B. (1969). Vertical heterogeneity in the water column of Abbot’s pond: I. The distribution of temperature and dissolved oxygen. *Journal of Ecology*, 57(2), 381. <https://doi.org/10.2307/2258386>

Muñoz-Sabater, J., Dutra, E., Agustí-Panareda, A., Albergel, C., Arduini, G., Balsamo, G., et al. (2021). ERA5-Land: A state-of-the-art global reanalysis dataset for land applications. *Earth System Science Data*, 13(9), 4349–4383. <https://doi.org/10.5194/essd-13-4349-2021>

Oertli, B., Biggs, J., Cérégino, R., Grillas, P., Joly, P., & Lachavanne, J.-B. (2005). Conservation and monitoring of pond biodiversity: Introduction. *Aquatic Conservation: Marine and Freshwater Ecosystems*, 15(6), 535–540. <https://doi.org/10.1002/aqc.752>

Oertli, B., Cérégino, R., Hull, A., & Miracle, R. (2009). Pond conservation: From science to practice. *Hydrobiologia*, 634(1), 1–9. <https://doi.org/10.1007/s10750-009-9891-9>

Oleksey, I. A., & Richardson, D. C. (2021). Climate change and teleconnections amplify lake stratification with differential local controls of surface water warming and deep water cooling. *Geophysical Research Letters*, 48(5), e2020GL090959. <https://doi.org/10.1029/2020GL090959>

Olson, D. M., & Dinerstein, E. (2002). The Global 200: Priority ecoregions for global conservation. *Annals of the Missouri Botanical Garden*, 89(2), 125–126. <https://doi.org/10.2307/3298564>

Padisák, J., & Reynolds, C. S. (2003). Shallow lakes: The absolute, the relative, the functional and the pragmatic. *Hydrobiologia*, 506–509(1–3), 1–11. <https://doi.org/10.1023/B:HYDR.0000008630.49527.29>

Palecki, M. A., Angel, J. R., & Hollinger, S. E. (2005). Storm precipitation in the United States. Part I: Meteorological characteristics. *Journal of Applied Meteorology*, 44(6), 933–946. <https://doi.org/10.1175/JAM2243.1>

Podgrajsek, E., Sahlée, E., & Rutgersson, A. (2014). Diurnal cycle of lake methane flux. *Journal of Geophysical Research*, 119(3), 236–248. <https://doi.org/10.1002/2013jg002327>

Rautio, M., Dufresne, F., Laurion, I., Bonilla, S., Vincent, W. F., & Christoffersen, K. S. (2011). Shallow freshwater ecosystems of the circum-polar Arctic. *Écoscience*, 18(3), 204–222. <https://doi.org/10.2980/18-3-3463>

R Core Team. (2020). The R project for statistical computing. Retrieved from <https://www.r-project.org/>

Read, J. S., Hamilton, D. P., Desai, A. R., Rose, K. C., MacIntyre, S., Lenters, J. D., et al. (2012). Lake-size dependency of wind shear and convection as controls on gas exchange. *Geophysical Research Letters*, 39(9), L09405. <https://doi.org/10.1029/2012GL051886>

Read, J. S., Hamilton, D. P., Jones, I. D., Muraoka, K., Winslow, L. A., Kroiss, R., et al. (2011). Derivation of lake mixing and stratification indices from high-resolution lake buoy data. *Environmental Modelling & Software*, 26(11), 1325–1336. <https://doi.org/10.1016/j.envsoft.2011.05.006>

Richardson, D. C., Holgerson, M. A., Farragher, M. J., Hoffman, K. K., King, K. B. S., Alfonso, M. B., et al. (2022). A functional definition to distinguish ponds from lakes and wetlands. *Scientific Reports*, 12(1), 10472. <https://doi.org/10.1038/s41598-022-14569-0>

Saari, G. N., Wang, Z., & Brooks, B. W. (2018). Revisiting inland hypoxia: Diverse exceedances of dissolved oxygen thresholds for freshwater aquatic life. *Environmental Science and Pollution Research*, 25(4), 3139–3150. <https://doi.org/10.1007/s11356-017-8908-6>

Sand-Jensen, K., Andersen, M. R., Martinsen, K. T., Borum, J., Kristensen, E., & Kragh, T. (2019). Shallow plant-dominated lakes – Extreme environmental variability, carbon cycling and ecological species challenges. *Annals of Botany*, 124(3), 355–366. <https://doi.org/10.1093/aob/mcz084>

Scheffer, M. (2004). *Ecology of shallow lakes*. Kluwer Academic Publishers.

Schmadel, N. M., Harvey, J. W., Schwarz, G. E., Alexander, R. B., Gomez-Velez, J. D., Scott, D., & Ator, S. W. (2019). Small ponds in headwater catchments are a dominant influence on regional nutrient and sediment budgets. *Geophysical Research Letters*, 46(16), 9669–9677. <https://doi.org/10.1029/2019GL083937>

Shatwell, T., Adrian, R., & Kirillin, G. (2016). Planktonic events may cause polymeric-dimictic regime shifts in temperate lakes. *Scientific Reports*, 6(1), 24361. <https://doi.org/10.1038/srep24361>

Singh, T. P., Singh, A. K., & Kaushik, N. D. (1994). Investigations of thermohydrodynamic instabilities and ground storage in a solar pond by simulation model. *Heat Recovery Systems and CHP*, 14(4), 401–407. [https://doi.org/10.1016/0890-4332\(94\)90043-4](https://doi.org/10.1016/0890-4332(94)90043-4)

Siver, P. A., Marsicano, L. J., Lott, A., Wagener, S., & Morris, N. (2018). Wind induced impacts on hypolimnetic temperature and thermal structure of Candlewood Lake (Connecticut, U.S.A.) from 1985–2015. *Geo: Geography and Environment*, 5(2), e00056. <https://doi.org/10.1002/geo2.56>

Song, K., Xenopoulos, M. A., Buttle, J. M., Marsalek, J., Wagner, N. D., Pick, F. R., & Frost, P. C. (2013). Thermal stratification patterns in urban ponds and their relationships with vertical nutrient gradients. *Journal of Environmental Management*, 127, 317–323. <https://doi.org/10.1016/j.jenvman.2013.05.052>

Spinu, V., Grolemond, G., Wickham, H., Lytle, I., Costigan, I., Law, J., et al. (2021). lubridate: Make dealing with dates a little easier (Version 1.7.10). Retrieved from <https://CRAN.R-project.org/package=lubridate>

Staehr, P. A., Christensen, J. P. A., Batt, R. D., & Read, J. S. (2012). Ecosystem metabolism in a stratified lake. *Limnology & Oceanography*, 57(5), 1317–1330. <https://doi.org/10.4319/lo.2012.57.5.1317>

Taguchi, V. J., Olsen, T. A., Natarajan, P., Janke, B. D., Gulliver, J. S., Finlay, J. C., & Stefan, H. G. (2020). Internal loading in stormwater ponds as a phosphorus source to downstream waters. *Limnology and Oceanography Letters*, 5(4), 322–330. <https://doi.org/10.1002/lo2.10155>

Therneau, T., Atkinson, B., & port, B. R., & (producer of the initial R., & maintainer 1999–2017). (2019). rpart: Recursive partitioning and regression trees (Version 4.1–15). Retrieved from <https://CRAN.R-project.org/package=rpart>

Torremorell, A., Bustigorry, J., Escaray, R., & Zagarese, H. E. (2007). Seasonal dynamics of a large, shallow lake, laguna Chascomús: The role of light limitation and other physical variables. *Limnologica*, 37(1), 100–108. <https://doi.org/10.1016/j.limno.2006.09.002>

Vachon, D., Langenegger, T., Donis, D., & McGinnis, D. F. (2019). Influence of water column stratification and mixing patterns on the fate of methane produced in deep sediments of a small eutrophic lake. *Limnology & Oceanography*, 64(5), 2114–2128. <https://doi.org/10.1002/lno.11172>

Vesala, T., Huotari, J., Rannik, Ü., Suni, T., Smolander, S., Sogachev, A., et al. (2006). Eddy covariance measurements of carbon exchange and latent and sensible heat fluxes over a boreal lake for a full open-water period. *Journal of Geophysical Research*, 111, D11101. <https://doi.org/10.1029/2005JD006365>

Watmuff, J. H., Charters, W. W. S., & Proctor, D. (1977). Solar and wind induced external coefficients for solar collectors. *Rev Int d'Heliothermique*, 2, 56.

Webb, J. R., Hayes, N. M., Simpson, G. L., Leavitt, P. R., Baulch, H. M., & Finlay, K. (2019). Widespread nitrous oxide undersaturation in farm waterbodies creates an unexpected greenhouse gas sink. *Proceedings of the National Academy of Sciences*, 116(20), 9814–9819. <https://doi.org/10.1073/pnas.1820389116>

Wilhelm, S., & Adrian, R. (2007). Impact of summer warming on the thermal characteristics of a polymeric lake and consequences for oxygen, nutrients and phytoplankton. *Freshwater Biology*, 53(0), 226–237. <https://doi.org/10.1111/j.1365-2427.2007.01887.x>

Winslow, L., Read, J. S., Woolway, R. I., Brentrup, J., Leach, T., Zwart, J., et al. (2019). rLakeAnalyzer: lake physics tools (Version 1.11.4.1). Retrieved from <https://cran.r-project.org/web/packages/rLakeAnalyzer/index.html>

Winslow, L. A., Read, J. S., Hansen, G. J. A., & Hanson, P. C. (2015). Small lakes show muted climate change signal in deepwater temperatures. *Geophysical Research Letters*, 42(2), 355–361. <https://doi.org/10.1002/2014GL062325>

Woolway, R. I., Jones, I. D., Hamilton, D. P., Maberly, S. C., Muraoka, K., Read, J. S., et al. (2015). Automated calculation of surface energy fluxes with high-frequency lake buoy data. *Environmental Modelling & Software*, 70, 191–198. <https://doi.org/10.1016/j.envsoft.2015.04.013>

Woolway, R. I., Meinson, P., Nöges, P., Jones, I. D., & Laas, A. (2017). Atmospheric stilling leads to prolonged thermal stratification in a large shallow polymictic lake. *Climatic Change*, 141(4), 759–773. <https://doi.org/10.1007/s10584-017-1909-0>

Woolway, R. I., & Merchant, C. J. (2019). Worldwide alteration of lake mixing regimes in response to climate change. *Nature Geoscience*, 12(4), 271–276. <https://doi.org/10.1038/s41561-019-0322-x>

Woolway, R. I., Verburg, P., Lengers, J. D., Merchant, C. J., Hamilton, D. P., Brookes, J., et al. (2018). Geographic and temporal variations in turbulent heat loss from lakes: A global analysis across 45 lakes. *Limnology & Oceanography*, 63(6), 2436–2449. <https://doi.org/10.1002/lno.10950>

Xia, Y., Mitchell, K., Ek, M., Sheffield, J., Cosgrove, B., Wood, E., et al. (2012). Continental-scale water and energy flux analysis and validation for the North American Land Data Assimilation System project phase 2 (NLDAS-2): 1. Intercomparison and application of model products. *Journal of Geophysical Research*, 117, D03109. <https://doi.org/10.1029/2011JD016048>